NEANDC (E) - 292 U Vol. V
INDC (Ger) - 32/LN + Special

PROGRESS REPORT ON NUCLEAR DATA RESEARCH IN THE FEDERAL REPUBLIC OF GERMANY

for the Period April 1, 1987 to March 31, 1988

June 1988

Edited by
S. Cierjacks
Kernforschungszentrum Karlsruhe
Institut für Material- und Festkörperforschung II

NEANDC (E) - 292 U Vol. V
INDC (Ger) - 32/LN + Special

PROGRESS REPORT ON NUCLEAR DATA RESEARCH IN THE FEDERAL REPUBLIC OF GERMANY

for the Period April 1, 1987 to March 31, 1988

June 1988

Edited by
S. Cierjacks
Kernforschungszentrum Karlsruhe
Institut für Material- und Festkörperforschung II

F O R E W O R D

This report has been prepared to promote the exchange of nuclear data research information between the Federal Republic of Germany and other member states of NEA and IAEA. It brings together progress reports from KfK Karlsruhe, KFA Jülich, the universities of Hannover, Köln, Mainz, München and Stuttgart, as well as from PTB Braunschweig and FIZ Karlsruhe. As in previous years, the emphasis in the work reported here is on measurements, evaluation and compilation of application-oriented nuclear data, such as those relevant to fission and fusion reactor technologies, development of intense spallation neutron sources, astrophysics research, cosmogenic and meteoritic investigations, production of medically important short-lived radioisotopes, etc.

Each contribution is presented under the laboratory heading where the work was done. When the work is relevant to requests in the World Request List for Nuclear Data, WRENDA 83/84 (INDC(SEC)-88/URSF), the corresponding request identification numbers are given in the headings of the respective contributions.

Karlsruhe, June 1988 S. Cierjacks

CONTENTS

KERNFORSCHUNGSZENTRUM KARLSRUHE
INSTITUT FÜR KERNPHYSIK II

1. Systematic Measurements of Differential Neutron Production Cross Sections for 585 MeV Protons

S. Cierjacks, Y. Hino[1], F. Raupp[2], L. Buth [3], D. Filges[4], P. Cloth[4], T.W. Armstrong[4]

Double differential cross sections $d^2\sigma/d\Omega\, dT_n$ for the production of neutrons from 585 MeV proton bombardment of C, Al, Fe, Nb, In, Ta, Pb, and U targets have been measured at emission angles of 30°, 90°, and 150° and for neutron kinetic energies between 0.9 and 585 MeV (all quantities in the laboratory system). The measured cross sections were compared with previous experimental results from other laboratories [1]. In Fig.1 the measured 30° cross sections from this work are shown. It can be seen that the experimental energy-dependent cross sections all reveal a clear two-component structure

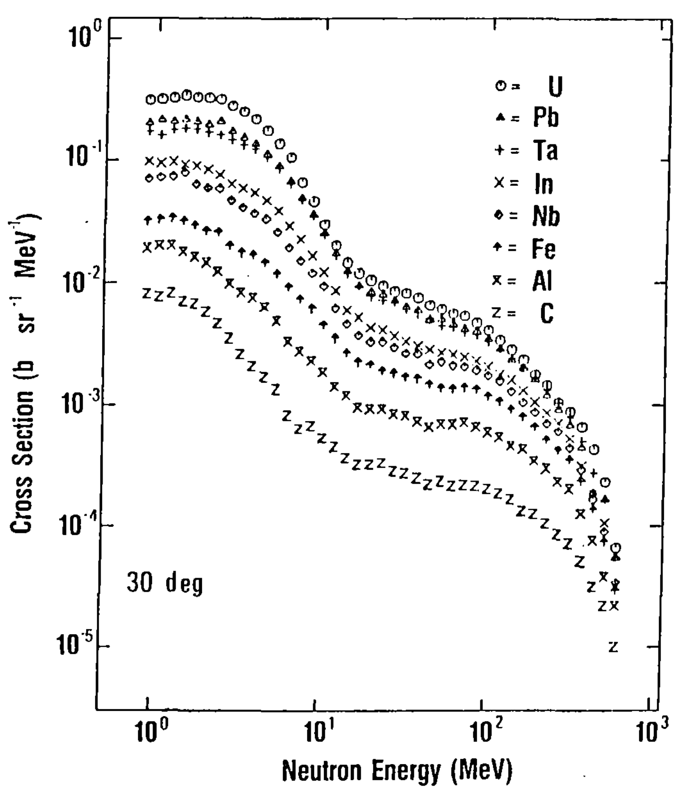

Fig. 1. Double differential neutron production cross sections for various elemental targets at 30° laboratory angle.

with contributions from intranuclear cascade reactions and evaporation processes in highly-excited residual nuclei. For heavy and medium weight nuclei the data in the evaporation region are indicative of an isotropic angular distribution in the zero-linear-momentum coordinate system. Data in the cascade energy region are strongly forward peaked, and the fraction of cascade neutrons increases with decreasing emission angle. This fraction also increases with decreasing mass number of the target nucleus.

2. Validation of Intranuclear Cascade-Evaporation Model Calculations for Neutron Production with 585 MeV Protons

D. Filges[4], P. Cloth[4], T.W. Armstrong[4], S. Cierjacks, Y. Hino[1], F. Raupp[2], L. Buth[3]

The intranuclear cascade-evaporation model of a high-energy nucleon- meson transport code has been used to calculate neutron production cross sections from non-elastic interactions of 585 MeV protons with C, Al, Fe, Nb, In, Ta, Pb, and U target nuclei at emission angles of 30°, 90°, and 150°. These model predictions were compared with the systematic measurements of the differential neutron production cross sections for neutrons with kinetic energies between 0.9 and 585 MeV [2]. In general, the model predicted approximately the correct neutron production in the evaporation region (better ~30%). But, in the high-energy region ($E_n \geq 20$ MeV) systematic discrepancies between measurements and model calculations were observed. The discrepancies increase rapidly with increasing neutron energy and increasing emission angle.

3. Neutron Fission Cross Sections of ^{235}U and $^{239,240}Pu$ in the Energy Range from 1 to 20 MeV

S. Cierjacks

The recent work on completion and reanalysis [3] of previously determined neutron fission cross sections or cross section ratios [4,5,6] has been continued. Especially data given in Refs.4,5 were previously only analyzed in preliminary form: For the absolute fission cross sections of ^{235}U only approximate detection efficiencies of our special proton recoil detectors have been used, because final efficiencies were not yet available at that time. In addition, shape measurements of $^{238}U/^{235}U$ and $^{239}Pu/^{235}U$ in Ref.4

were normalized arbitrarily at 14 MeV due to the lack of final mass determinations. Concerning the fission cross sections of ^{239}Pu and the fission cross section ratios of $^{239}Pu/^{235}U$ determined in the work of Ref.6, doubts about the accuracy of the energy scale have been raised in a recent ENDL evaluation [7]. To investigate this problem, a reanalysis of the corresponding raw data is underway.

---

[1] Now at Electrotechnical Laboratory, 114 Umezono, Ibaraki, Japan

[2] Now at Elektronik System Gesellschaft, Munich, Fed. Rep. of Germany

[3] Kernforschungszentrum Karlsruhe, Institut für Neutronenphysik und Reaktortechnik

[4] Institut für Reaktorentwicklung, Kernforschungsanlage Jülich

References

[1] S. Cierjacks, Y. Hino, F. Raupp, L. Buth, D. Filges, P. Cloth and T.W. Armstrong; Systematics of angular-dependent neutron production by 585 MeV protons on targets with $12 \leq A \leq 238$: Differential cross section measurement; Phys. Rev. C36 (1987) 1976

[2] D. Filges, P. Cloth, T.W. Armstrong, S. Cierjacks, Y. Hino, and L. Buth; Systematics of angular-dependent neutron production by 585 MeV protons on targets with $12 \leq A \leq 238$: Validation of intranuclear cascade-evaporation model calculations; Phys. Rev. C36 (1987) 1988

[3] S. Cierjacks; Neutron fission cross sections of ^{235}U, ^{239}Pu, and ^{240}Pu and fission cross section ratios of $^{239}Pu/^{235}$ and $^{240}Pu/^{235}U$; NEANDC Progress Report, NEANDC(E)-282U, Vol.V, 1988, p. 3

[4] B. Leugers, S. Cierjacks, P. Brotz, D. Erbe, D. Gröschel, G. Schmalz and F. Voss; The ^{235}U and the ^{238}U neutron-induced fission cross sections relative to the H(n,p) cross section; Argonne National Laboratory Report, ANL-78-90, 1976, p. 246

[5] S. Cierjacks, B. Leugers, K. Kari, P. Brotz, D. Erbe, D. Gröschel, G. Schmalz and F. Voss; Measurements of neutron-induced fission cross section ratios at the Karlsruhe isochronous cyclotron; Argonne National Laboratory Report, ANL-78-90, 1976, p. 94

[6] K. Kari; Messung der Spaltquerschnitte von ^{239}Pu und ^{240}Pu relativ zum Spaltquerschnitt von ^{235}U und zum Streuquerschnitt H(n,p) im Neutronenenergiebereich zwischen 0.5 und 20 MeV; Kernforschungszentrum Karlsruhe Report, KfK 2673, 1978; and K. Kari and S. Cierjacks; Measurements of the fast fission cross sections of ^{239}Pu and ^{240}Pu; Proc. Int. Conf. on Neutron Physics and Nuclear Data, Harwell 1978, p. 905

[7] R.J. Howerton and R.M. White; A reevaluation for ENDL of $\sigma(n,f)$ and ν_p for ^{235}U and ^{239}Pu from 100 keV to 20 MeV; Lawrence Livermore National Laboratory Report, UCID-19973, 1984

KERNFORSCHUNGSZENTRUM KARLSRUHE
INSTITUT FÜR KERNPHYSIK III

1. ACTIVATION OF SHORT LIVED ISOTOPES - A MEASUREMENT OF THE $^{107,109}Ag$ CAPTURE CROSS SECTIONS

H. Beer, F. Voss, F. Käppeler, G. Rupp

A new setup for activation measurements on isotopes with short-lived residual activities (> 1 sec) has been tested, consisting of a fast sample changer and a Ge(Li) detector (154 cm^3, 2.6 keV resolution at 1.332 MeV). Neutrons are produced in the $^7Li(p,n)^7Be$ reaction at E_p = 1912 keV, kinematically collimated with an opening angle of 120°. The Ge(Li) detector is located outside the neutron beam and shielded by lead, Cd sheets, and boron loaded paraffin.

During the irradiation phase, the proton beam current and the neutron flux are monitored; in addition, the neutron flux is recorded as a function of time. Data accumulation from the Ge(Li) detector is blocked by a signal for the analog-to-digital converter. During the counting phase, neutron production is turned off by a beam stop and the induced activities are recorded via the Ge(Li) detector.

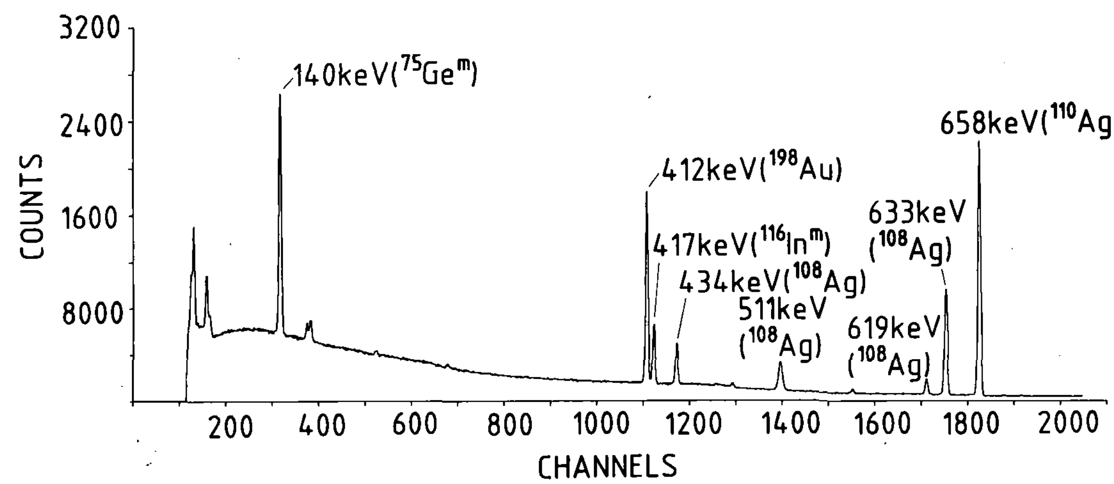

Fig. 1 The Ge(Li) spectrum accumulated in 640 activation cycles of a natural silver sample.

The experimental setup is designed for a determination of the $^{22}Ne(n,\gamma)^{23}Ne$ (38sec) cross section and was tested by a measurement of the cross sections for $^{107}Ag(n,\gamma)^{108}Ag$ (2.41 min) and $^{109}Ag(n,\gamma)^{110}Ag$ (24.6 sec). First results are presented in Fig. 1. The plotted spectrum was accumulated in 640 cycles, each consisting of 26 sec intervals for irradiation and counting, respectively. Besides the gamma activities from the silver sample and the gold standard, prominent background lines from ^{116m}In and ^{75m}Ge were also observed, resulting from capture of scattered neutrons in the Ge(Li) detector.

The result on $^{109}Ag(n,\gamma)^{110}Ag$ (24.6 sec) was used to estimate the sensitivity of the setup for the $^{22}Ne(n,\gamma)$ reaction: With a 6mg ^{22}Ne sample the cross section limit would be 0.3 mb.

2. NEUTRON CAPTURE IN $^{185,187}Re$ - A MEASUREMENT AT kT = 25 keV

F. Käppeler, Z.Y. Bao*, M. Heil

The interpretation of the chronometric pair ^{187}Re - ^{187}Os has been shown (1,2,3) to be complicated by various effects, e.g. electron capture in ^{187}Os which may invalidate the local approximation commonly used in analyses of this clock. The above problem is related to the s-process mass flow through the branching at A = 185, 186. Apart from the difficult question of the stellar neutron capture rate of ^{187}Os (4), the status of some other involved cross sections is also not satisfactory (5).As long as the experimental data in this mass range are incomplete, calculations of the cross sections for the unstable branching isotopes ^{185}W and ^{186}Re cannot be based on reliable systematics.

To improve this situation, we started a measurement on $^{185,187}Re$. The cross sections of both isotopes can be derived simultaneously by activation of a natural rhenium sample. The decay of the product nuclei $^{186,188}Re$ yields gamma-rays of 137 and 155 keV, respectively. The activations are performed in the quasi stellar neutron spectrum obtained with the $^{7}Li(p,n)^{7}Be$ reaction, corresponding to a thermal energy of kT=25 keV. Fig. 1 shows the gamma-ray spectrum measured after activation of a 14.7 mg sample for 5.4 h. The background due to beta decay electrons appears rather high because the related gamma-ray intensities are relatively weak. Preliminary results from a first series of activations indicates a significantly smaller cross section for ^{187}Re as compared to previous data (4).

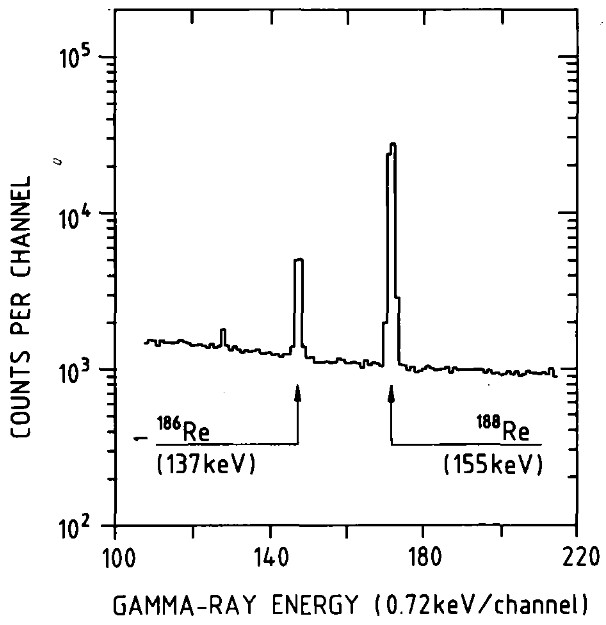

Fig. 1
Gamma-ray spectrum recorded after activation of a natural Re sample

(1) J. Conrad, H.D. Zeh, Z. Naturforsch. 33a (1978) 887
(2) K. Yokoi, K. Takahashi, M. Arnould, Astron.Astrophys. 117(1983)6
(3) M. Arnould, K. Takahashi, K. Yokoi, Astron.Astrophys. 137(1984)51
(4) R.R. Winters, R.F. Carlton, J.A. Harvey, N.W. Hill,Phys. Rev. C34 (1986)840
(5) Z.Y. Bao, F. Käppeler, Atomic Data and Nuclear Data Tables 36 (1987)411

* Institute of Atomic Energy, Academia Sinica, Beijing, Peoples Republic of China

3. THE NEUTRON CAPTURE CROSS SECTION OF ^{197}AU – A STANDARD FOR STELLAR NUCLEOSYNTHESIS*

W. Ratynski⁺, F. Käppeler

We have measured the neutron capture cross section of gold using the ^{7}Li (p, n)^{7}BE reaction for neutron production. This reaction does not only provide the integrated neutron flux via the ^{7}Be activity of the target, but allows also for the simulation of a Maxwellian neutron energy spectrum at kT = 25 keV. As this spectrum is emitted in a forward cone of 120° opening angle, the cross section can be measured in good geometry and independent of any other standard. Systematic uncertainties were studied experimentally in a series of activations. The final stellar cross section at kT = 25 keV was found to be 648 ± 10 mb, and extrapolation to the common s-process termperature kT = 30 keV yields 582 ± 9 mb. This result is used for renormalization of a number of cross sections which had been measured relative to gold. Figure 1 shows the present result compared to previous measurements.

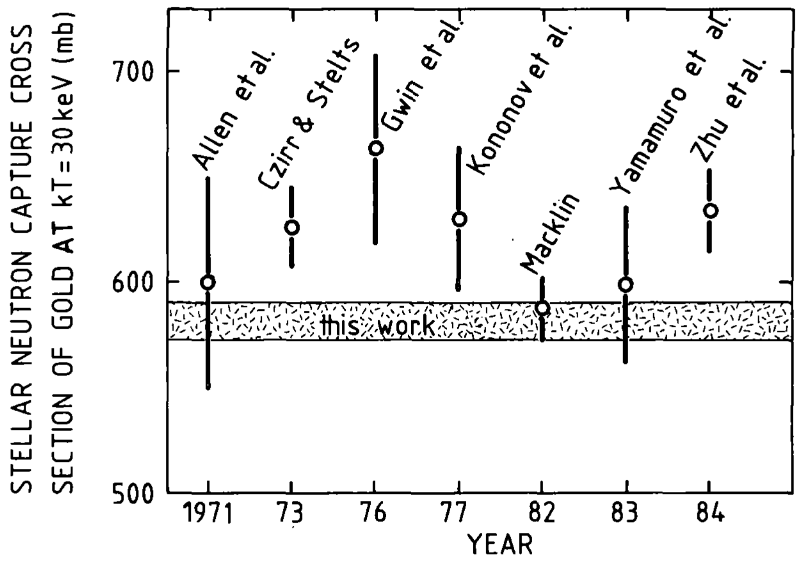

Fig. 1 Comparison between previous measurements and the present result.

* Phys. Rev. C 37 (1988) 595 - 604

+On leave from Institute for Nuclear Studies. Swierk, Poland.

KERNFORSCHUNGSZENTRUM KARLSRUHE
INSTITUT FÜR NEUTRONENPHYSIK UND REAKTORTECHNIK

1. Nuclear Data Evaluation

1.1 Evaluation of Neutron Cross Sections for ^{238}U in the Unresolved Resonance Region

F.H. Fröhner

A joint JEF-2 evaluation for ^{238}U+n is in progress at Harwell and Karlsruhe. At KfK the unresolved resonance region between about 10 and 500 keV has been studied extensively with the Hauser-Feshbach program FITACS, which permits simultaneous fitting of average total, capture and inelastic scattering cross sections by adjustment of strength functions, distant-level parameters and average radiation widths for all s-, p-, d- and f-wave channels. As reported last year [1] the fits indicated that the ratio of s-wave radiation width, 23.5 ± 0.3 meV, to mean level spacing, 21.5 ± 1.5 eV, inferred from resolved resonance parameters, was apparently several percent too high. In the meantime the ongoing analysis of resolved resonances at Harwell yielded 23.0 meV for the mean radiation width [2]. Furthermore, a statistical analysis of the new Harwell resonance parameters was performed at KfK with the STARA code [3]. It turned out that the older analyses were affected by incorrect spin and parity assignments for weak levels. Therefore, only levels with more than 99 % s-wave probability, as inferred from their $g\Gamma_n$ values, were retained for the simultaneous estimation of level density and strength function from level positions and neutron widths. Representative results are given in Table 1. The new mean level spacing is about 22.8 eV. Together with the new radiation width of 23.0 meV it is now reasonably consistent with the capture cross section obtained in the unresolved region.

Table 1: Maximum-likelihood estimates of level statistics from preliminary JEF-2 resonance parameters below 4 keV

Energy Range (keV)	Retained Levels	Missing Levels	Strength Function (10^{-4})	Mean Spacing (eV)
0 - 1	39	7	$0.96^{+.26}_{-.16}$	22.7 ± 1.6
0 - 2	70	21	$1.07^{+.19}_{-.14}$	22.5 ± 1.0
0 - 3	99	29	$1.20^{+.18}_{-.13}$	23.4 ± 0.6
0 - 4	130	53	$1.20^{+.14}_{-.11}$	22.5 ± 0.9

Another inconsistency existed last year between the $^{238}U(n,\gamma)$ cross section recommended for JEF-2 and the preliminary ENDF/B-VI evaluation: the latter was several percent lower. This was disturbing because the ENDF evaluation was performed for all standard reactions simultaneously - $^{1}H(n,n)$, $^{6}Li(n,t)$, $^{10}B(n,\alpha)$, $^{197}Au(n,\gamma)$, $^{235}U(n,f)$, $^{238}U(n,\gamma)$, $^{238}U(n,f)$ and $^{239}Pu(n,f)$ - while the JEF evaluation was restricted to ^{238}U but fitted data in all open channels simultaneously with the exact (GOE) level-statistical model [4], with rigorous (Bayesian) inclusion of a-priori information from the resolved resonance region and from the optical model. Recently, however, the ENDF evaluation has been modified and now agrees within error bars with the JEF-2 recommendation, at least up to the third inelastic threshold at about 310 keV [2].

References

[1] F.H. Fröhner, Progress Report EANDC(E)-282 vol. V (1988) p. 11

[2] M. Sowerby, private communication

[3] F.H. Fröhner, IAEA Meeting on Uranium and Plutonium Isotope Resonance Parameters, INDC(NDS)-129/GJ, Vienna (1981), p. 103

[4] F.H. Fröhner, IAEA Meeting on Nuclear Models for Fast Neutron Nuclear Data Evaluation, Beijing 1987 (to be published by IAEA)

1.2 Watt Spectrum Fit to ^{252}Cf Prompt Fission Neutron Data

F.H. Fröhner

Data from ten recent (post-1982) measurements of the ^{252}Cf prompt fission neutron spectrum have been fitted with four types of theoretical models: (1) a Maxwell spectrum, (2) a Watt spectrum, (3) a superposition of two Watt spectra representing a typical pair of fission fragments, and (4) a relativistic generalisation of (3). Instrumental resolution has been accounted for by exploitation of the fact that the Watt spectrum is mathematically identical with the free-gas Doppler broadening kernel, so that instrumental broadening is equivalent to a slight rise in nuclear temperature. The Maxwell spectrum was found inadequate, as expected, but a Watt spectrum with parameters

$$T_W = 1.175 \pm 0.005 \text{ MeV}, \; E_W = 0.359 \pm 0.009 \text{ MeV}$$

fits all data well up to 20 MeV, except for those above 17 MeV from one set, with a chi-square that indicates no need for a more refined model (Figs. 1, 2). The superposition of two Watt spectra and the relativistic generalisation do not improve the fit [1]. When Mannhart's [2] evaluated point data became available they were subjected to the same fitting procedure (except for the resolution broadening). The Watt spectrum obtained had the parameters

$$T_W = 1.174 \pm 0.008 \text{ MeV}, \; E_W = 0.361 \pm 0.014 \text{ MeV} .$$

In spite of the slightly different data base and correction procedures this agrees well with the result given above.

References

[1] F.H. Fröhner, IAEA Meeting on Nuclear Models for Fast Neutron Nuclear Data Evaluation, Beijing 1987 (to be published by IAEA)

[2] W. Mannhart, Proc. Meeting on Properties of Neutron Sources, Leningrad 1986, IAEA-TECDOC-410 (1987)

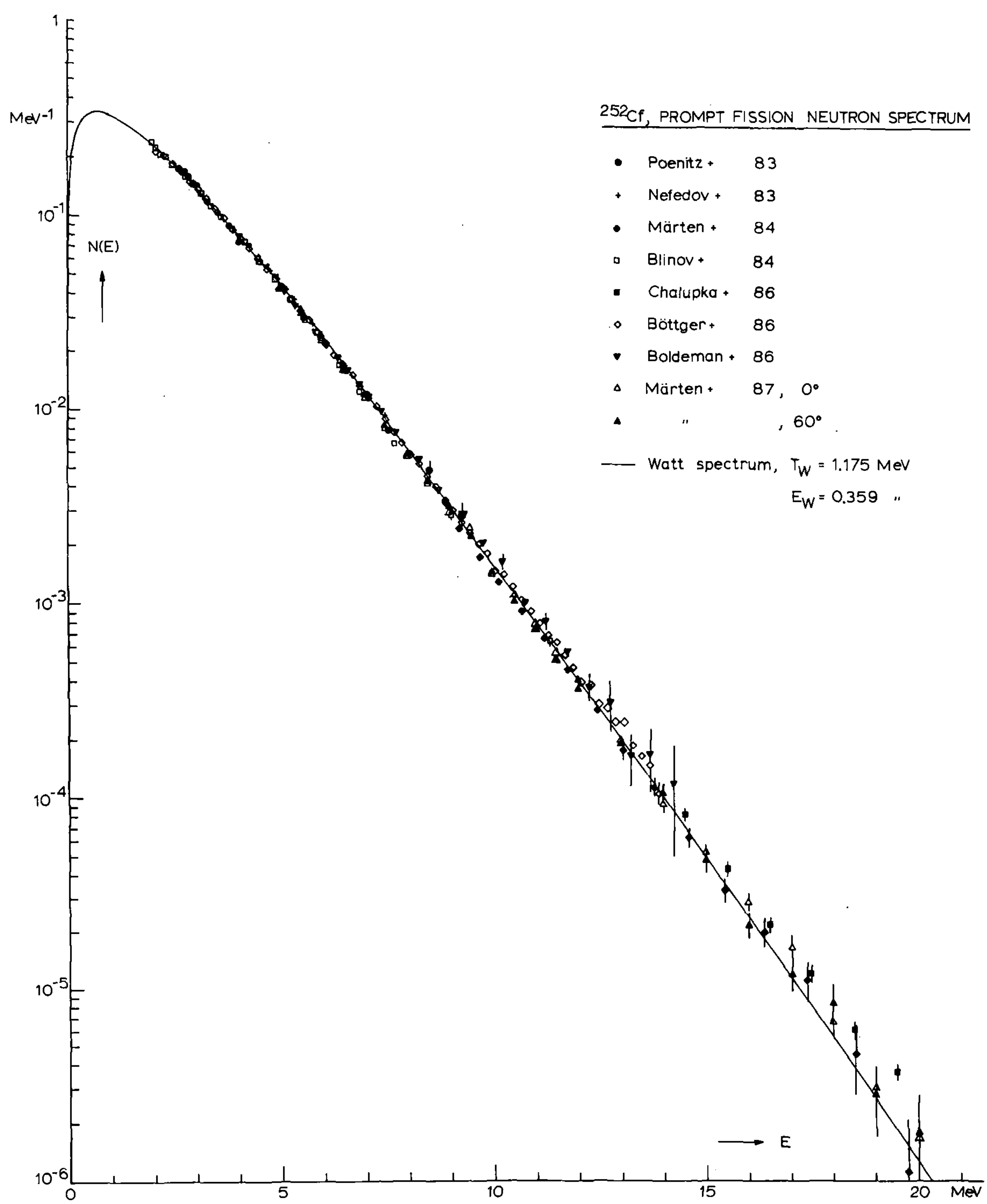

Fig. 2 - Utilised data above 3 MeV (error bars are mostly omitted for clarity) and adjusted Watt distribution, showing quality of fit in the tail of the fission neutron spectrum (from Ref. 1).

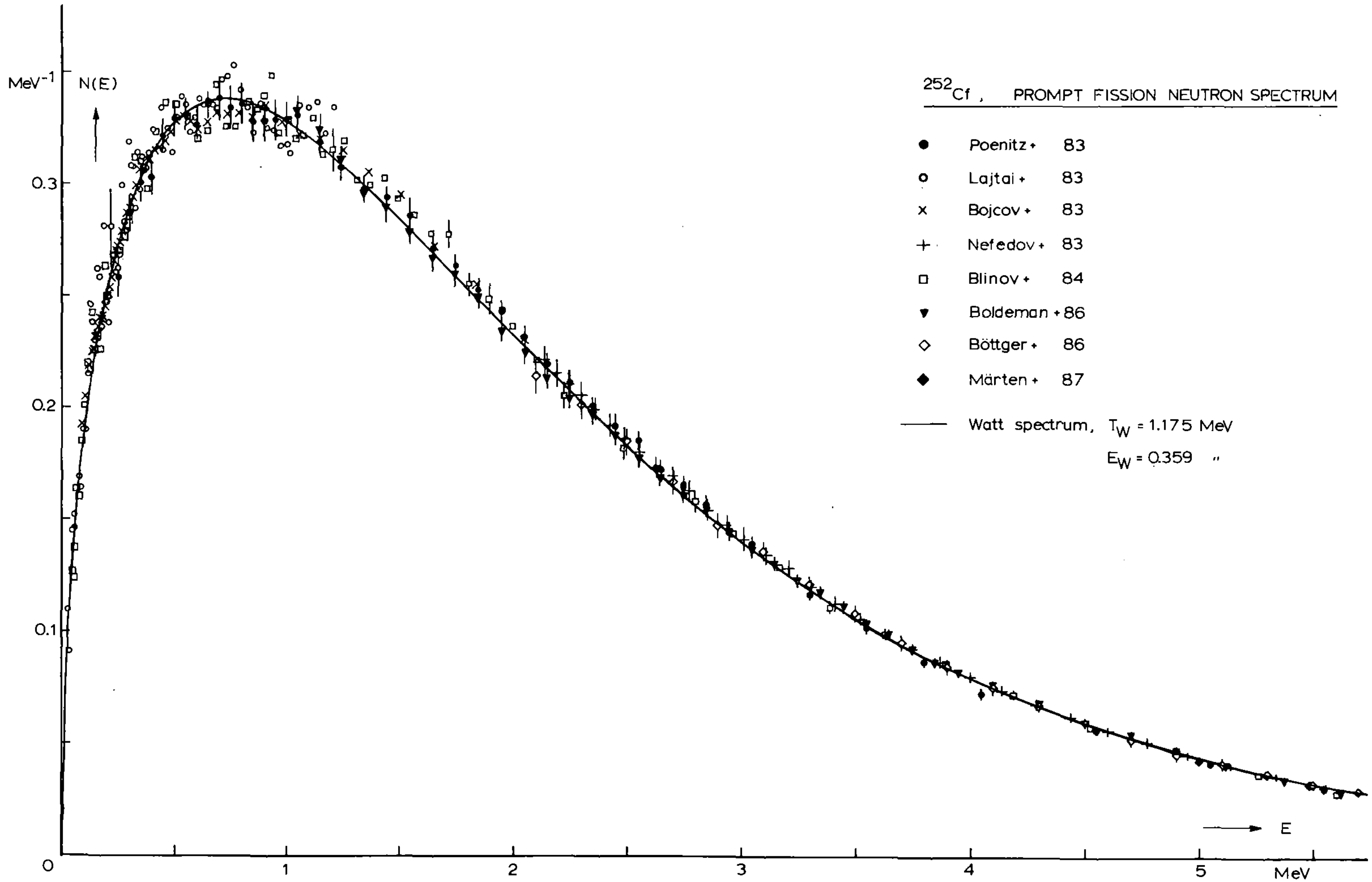

Fig. 1 - Utilised data below 5.7 MeV (error bars are mostly omitted for clarity) and adjusted Watt spectrum, showing quality of fit in the practically most important part of the fission neutron spectrum. (from Ref. 1).

1.3 Calculation of Secondary Neutron Spectra for Continuum Inelastic Scattering of Neutrons by Copper

I. Broeders, C. Broeders and E. Stein

The nuclear data libraries that are being used at KfK for fusion reactor blanket calculations contain copper data from ENDF/B-IV. In these data there is a lack of high-energy neutrons in the neutron emission spectra. The same is true for ENDF/B-V [1]. The reason is probably that pre-equilibrium reactions were not adequately taken into account in the evaluation.

Therefore, the emission spectra for continuum inelastic scattering were recalculated for incident neutron energies between 5 and 20 MeV with M. Blann's geometry-dependent hybrid model [2]. At an incident energy of 14.1 MeV our results could be compared to a recent model-free evaluation of experimental data by A. Pavlik and H. Vonach [3]. The agreement is quite reasonable. The new emission spectra exceed the old evaluations considerably above 7 MeV of secondary neutron energy. The influence of the newly calculated data on integral calculations was studied for a copper sphere with a 14 MeV neutron source in the centre.

References

[1] D.M. Hetrick, D.C. Larson and C.Y. Fu, Proc. Internat. Conf. on Nuclear Cross Sections and Technol., Knoxville (1979)

[2] M. Blann, Nucl. Phys. A213 (1973) 570;
H. Jahn, Report KfK 3646 (1984)

[3] H. Vonach, private communication

INSTITUT FÜR CHEMIE (1): NUKLEARCHEMIE
KERNFORSCHUNGSANLAGE JÜLICH

1. Neutron Data

1.1 (n,t) Cross Sections on Light Nuclei

A. Suhaimi, R. Wölfle, S.M. Qaim, G. Stöcklin

In continuation of our studies on (n,t) reactions on light mass nuclei [cf. 1-3] we measured the excitation function of the $^{14}N(n,t)^{12}C$ reaction over the energy range of 5 to 10.6 MeV [4]. The results are shown in Fig. 1. The cross sections lie between 11 and 30 mb and have an uncertainty of 14 to 21%. The excitation function shows fluctuation over the whole invetigated energy range; it is attributed to the decay properties of the excited nuclear levels involved [cf. 4,5].

The cross section of the $^{10}B(n,t)2\alpha$ process was measured at thermal neutron energy [5]. Irradiations were done in a pure thermal column of the research reactor DIDO ($\emptyset_{th}/\emptyset_f = 10^4$) and the technique of tritium separtion and counting was the same as in previous works from this Institute. The cross section was found to be 12.0 ± 2.5 mb. We feel that the long standing discrepancy about this cross section is now solved.

Investigations were carried out on the $^{9}Be(n,t)^{7}Li$ reaction with the aim to perform integral tests on the (n,t) excitation function measured recently [3]. Integral cross sections were measured using d/Be breakup neutrons (E_d = 17.5 to 30.0 MeV). The data agree within 20% with the average cross sections [5] derived from the excitation function of this reaction and the neutron spectral distributions .

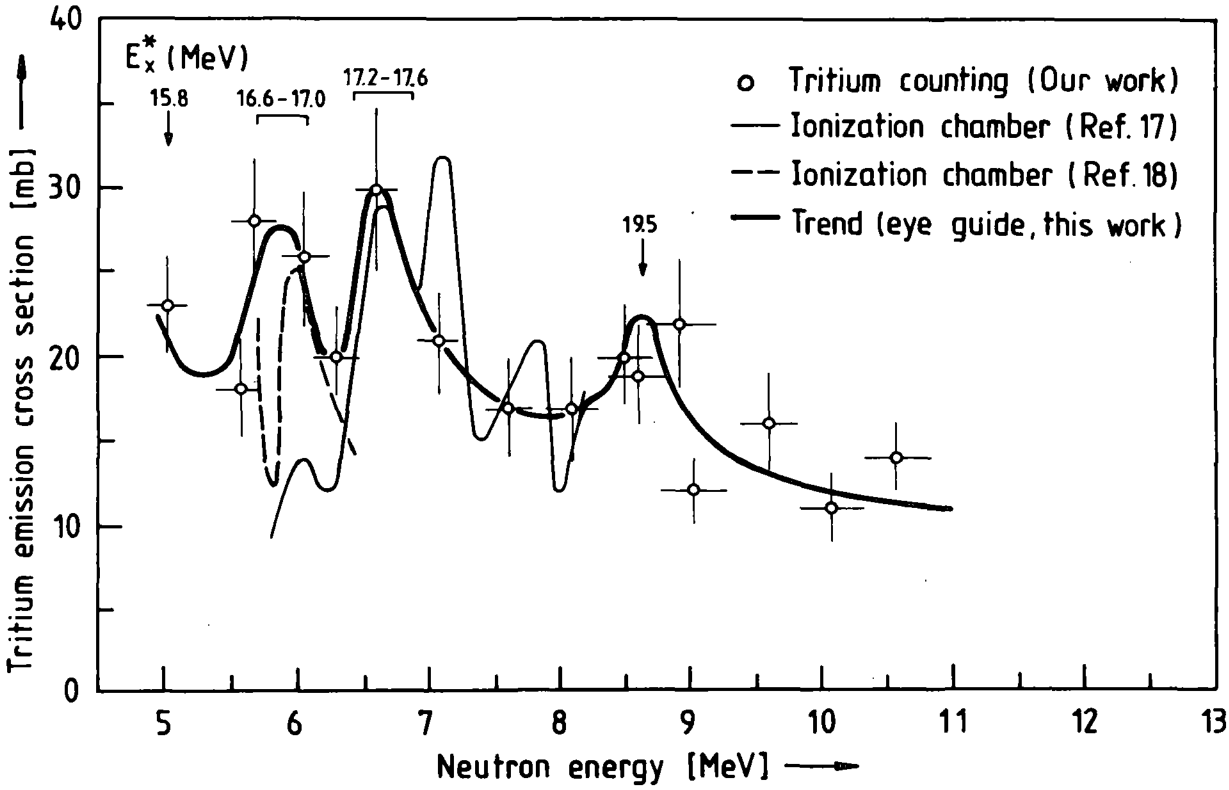

Fig. 1 Excitation function of $^{14}N(n,t)^{12}C$ reaction. The energy regions of the excited nucleus $^{15}N^*$ shown correspond to groups of levels decaying by triton emission [cf. 4,5].

1.2 Activation Cross Sections for Fusion Reactor Technology

R. Wölfle, A. Mannan, M. Ibn Majah, S.M. Qaim,

G. Stöcklin

(Relevant to request identification numbers: 724040F, 724041F, 724042F, 724049F, 742133R)

In continuation of our radiochemical measurements on activation products we completed systematic studies on the $^{93}Nb(n,2n)^{92m}Nb$ and $^{93}Nb(n,\alpha)^{90m,g}Y$ reactions from threshold up to 10.6 MeV [6]. The cross sections for the $^{93}Nb(n,2n)^{92m}Nb$ reaction should provide a useful data base for dosimetry purposes. The data for the $^{93}Nb(n,\alpha)^{90m+g}Y$ process give the total helium formation cross section. The results are shown in Fig. 2. Statistical model calculations (incorporating precompound effects) done at Vienna describe both the magnitude and the shape of the excitation function well.

Measurements of (n,p), (n,α) and (n,2n) reactions on several isotopes of zirconium were carried out in the energy range of 4 to 10.6 MeV. Analysis of the data is in progress. Zirconium is an important reactor material but the data base up to 13 MeV is very weak. Our results should provide some useful information.

Excitation function measurements on the reactions $^{93}Nb(n,\alpha)^{90m,g}Y$, $^{139}La(n,\alpha)^{136}Cs$ and $^{181}Ta(n,p)^{181}Hf$ in the neutron energy range of 12.5 to 20 MeV in collaboration with CBNM Geel (H. Liskien, R. Widera) were completed [7]. These reactions serve as good monitors.

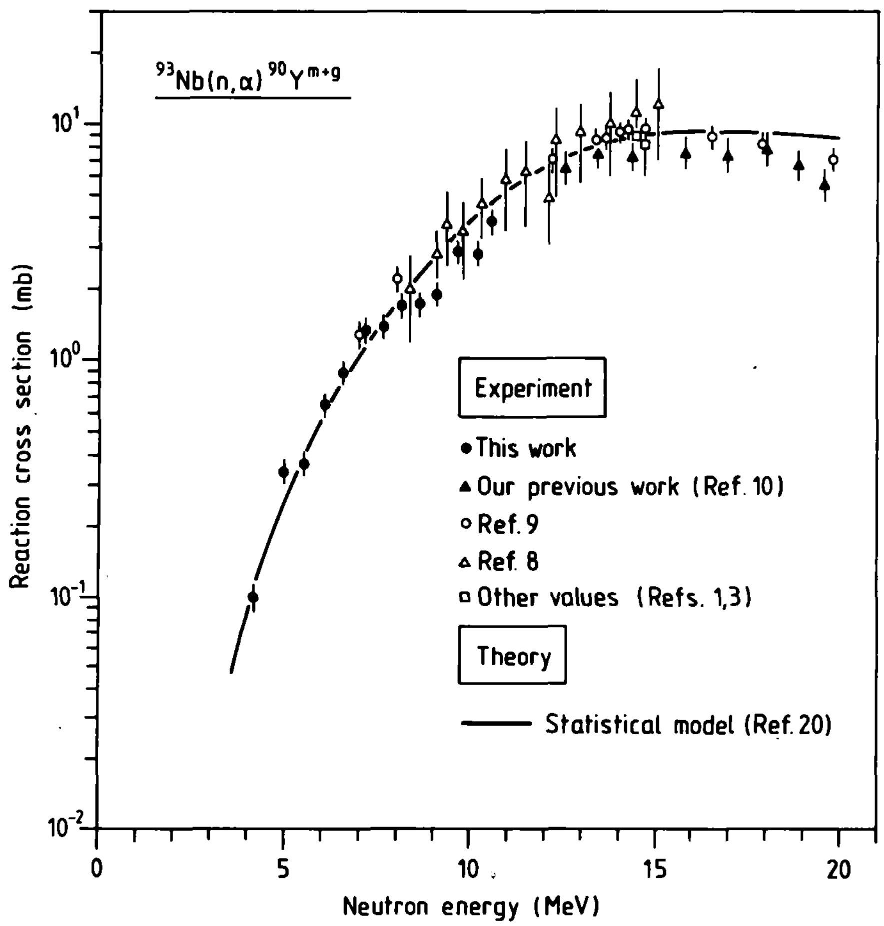

Fig. 2 Excitation function of $^{93}Nb(n,\alpha)^{90m+g}Y$ process [cf. 6,7].

2. Charged Particle Data for Radioisotope Production

A. Mushtaq, F. Tárkányi, M.S. Sutisna, B. Scholten,
S.M. Qaim, G. Stöcklin

In continuation of our studies on the production of medically important short-lived β^+-emitting and single photon emitting radioisotopes we measured excitation functions relevant to the formation of ^{73}Se, ^{82}Sr(^{82}Rb), ^{38}K and ^{123}I. In the case of ^{73}Se ($T_{1/2}$ = 7.1 h) (p,xn) and (d,xn) reactions on As were investigated [8]. The results for the $^{75}As(p,xn)^{72,73,75}Se$ processes are shown in Fig. 3. The optimum energy range for the production of ^{73}Se via the (p,3n) process is E_p = 40 → 30 MeV. The thick target yield of ^{73}Se amounts to 38 mCi/μAh and the $^{72,75}Se$ impurities to < 0.1%. For the (d,4n) process the optimum energy range was found to be E_d = 45 → 33 MeV. The thick target yield of ^{73}Se amounts to 17.6 mCi/μAh and the level of $^{72,75}Se$ to < 0.2%. The $^{75}As(p,3n)^{73}Se$ reaction is therefore more suitable for the production of ^{73}Se.

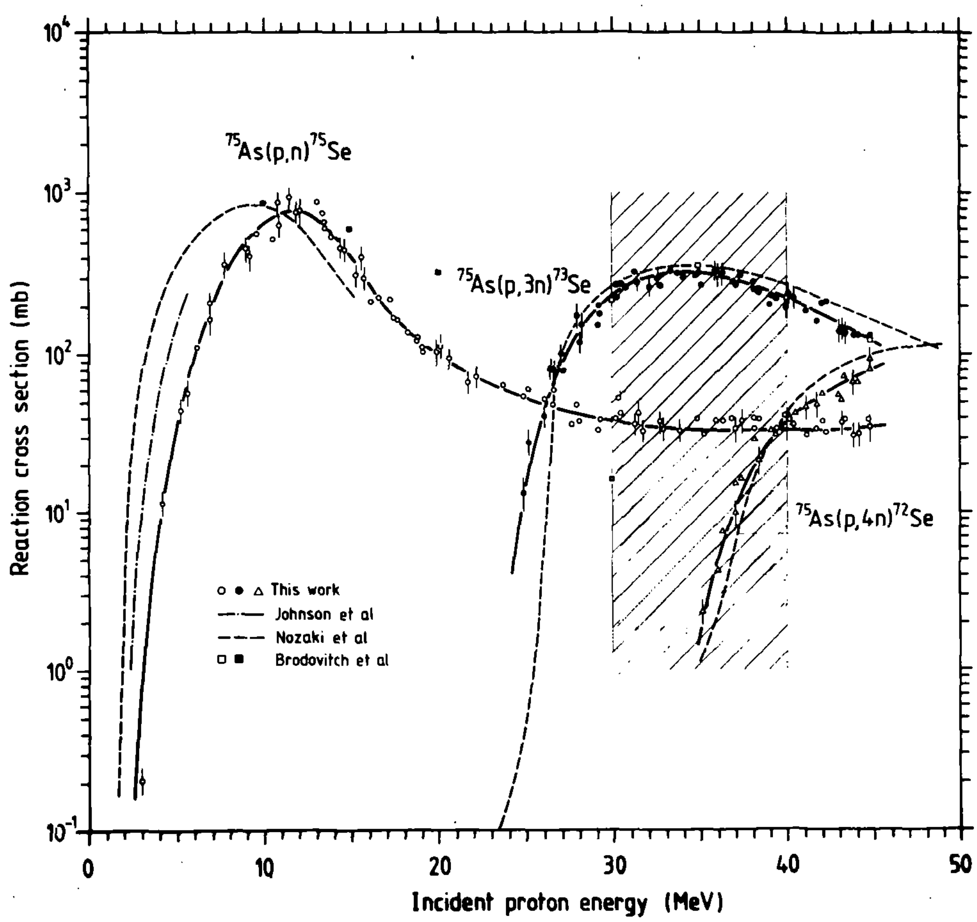

Fig. 3 Excitation functions of $^{75}As(p,xn)^{72,73,75}Se$ reactions. The optimum energy range for the production of ^{73}Se (E_p = 40 → 30 MeV) is shown [8].

Cross section measurements relevant to the production of ^{82}Sr (parent of β^+ emitting 1.2 min ^{82}Rb) via the $^{nat}Kr(^3He,xn)^{82}Sr$ process, reported earlier [9], were extended to enriched ^{82}Kr and ^{83}Kr as target gases [10]. It was found that the major process of interest for the production of ^{82}Sr at a compact cyclotron is the $^{82}Kr(^3He,3n)^{82}Sr$ reaction.

In connection with the production of short-lived ^{38}K ($T_{1/2}$ = 7.6 min) excitation functions were measured for the $^{35}Cl(\alpha,n)^{38}K$ and $^{35}Cl(\alpha,\alpha n)^{34m}Cl$ reactions up to 26 MeV [11]. Cross section data and calculated thick target yields show that the optimum energy range for the production of ^{38}K is E_α = 22.5 → 7 MeV; the thick target yield of ^{38}K amounts to 5.5 mCi/μA·15 min and the level of ^{34m}Cl is < 0.2%.

With a view to investigating the production of ^{123}I ($T_{1/2}$ = 13.1 h) at a small cyclotron (e.g. a Baby Cyclotron) we measured the excitation function of the $^{123}Te(p,n)^{123}I$ reaction using highly enriched ^{123}Te as target material. The results are shown in Fig. 4. The maximum of the excitation function of the

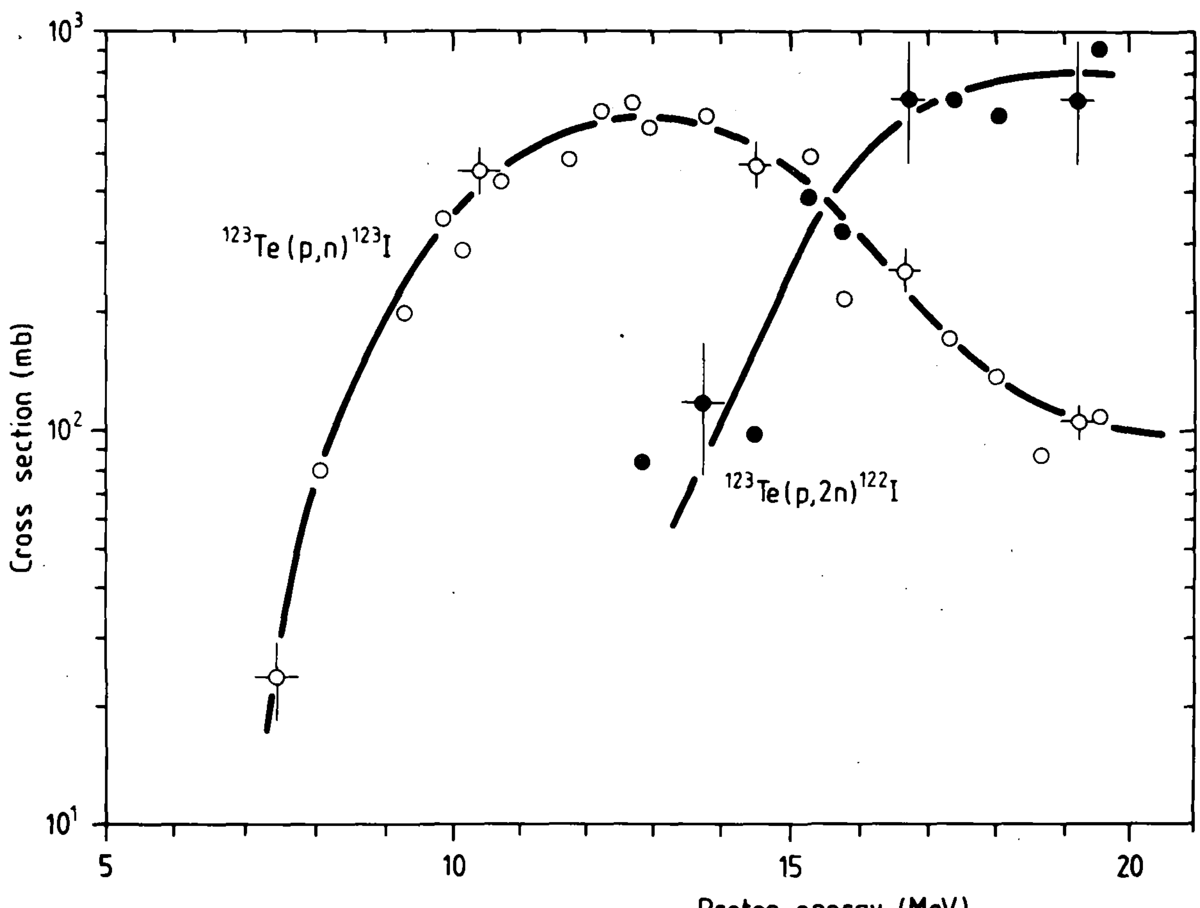

Fig. 4 Excitation functions of $^{123}Te(p,xn)^{123,122}I$ reactions measured on 85.4% enriched ^{123}Te, extrapolated to 100% enrichment.

$^{123}Te(p,n)^{123}I$ reaction lies at about 12.5 MeV and the cross section at the maximum amounts to about 700 mb. The product of the $^{123}Te(p,2n)^{122}I$ reaction is very short-lived ($T_{1/2}$ = 3.6 min) and is of little significance in the production process. The optimum energy range for the production of ^{123}I via the $^{123}Te(p,n)^{123}I$ reaction is E_p = 14.5 → 11 MeV. The calculated thick target yield of ^{123}I amounts to 7.3 mCi/μAh. The levels of the radioactive impurities ^{124}I, ^{126}I and ^{130}I depend directly on the % of the ^{124}Te, ^{126}Te and ^{130}Te, respectively, in the enriched ^{123}Te used. For the highest commercially available ^{123}Te-enrichment of 91%, the ^{124}I, ^{126}I and ^{130}I impurities are 0.55, 0.05 and 0.98%, respectively.

References

[1] A. Suhaimi, R. Wölfle, S.M. Qaim, G. Stöcklin: Measurement of $^{10}B(n,t)2\alpha$ reaction cross section in the energy range of 2.5 to 10.6 MeV: Diffusion of tritium in boron carbide, Radiochimica Acta 40 (1986) 113

[2] S.M.Qaim, R. Wölfle: $^{7}Li(n,n't)^{4}He$ reaction cross section via tritium counting, Nucl. Sci. Eng. 96 (1987) 52

[3] H. Liskien, R. Widera, R. Wölfle, S.M. Qaim: Experimentally determined excitation function for the $^{9}Be(n,t)$ reaction, Nucl. Sci. Eng. 98 (1988) 266

[4] A. Suhaimi, R. Wölfle, S.M. Qaim, P. Warwick, G. Stöcklin: Measurement of $^{14}N(n,t)^{12}C$ reaction cross section in the energy range of 5.0 to 10.6 MeV, Radiochimica Acta, in press

[5] S.M. Qaim, A. Suhaimi, R. Wölfle, G. Stöcklin: Measurement of (n,t) cross sections on light nuclei, Proc. Int. Conf. on Nuclear Data, Mito, Japan, May 1988, in press

[6] A. Mannan, S.M. Qaim: Activation cross section and isomeric cross-section ratio for the $^{93}Nb(n,\alpha)^{90m,g}Y$ reaction, Phys. Rev. C, submitted

[7] R. Wölfle, A. Mannan, S.M. Qaim, H. Liskien, R. Widera: Excitation functions of $^{93}Nb(n,2n)^{92m}Nb$, $^{93}Nb(n,\alpha)^{90m,g}Y$, $^{139}La(n,\alpha)^{136}Cs$ and $^{181}Ta(n,p)^{181}Hf$ reactions in the energy range of 12.5 to 19.6 MeV, Int. J. Appl. Radiat. Isotopes, in press

[8] A. Mushtaq, S.M. Qaim, G. Stöcklin: Production of ^{73}Se via (p,3n) and (d,4n) reactions on arsenic, Int. J. Appl. Radiat. Isotopes, in press

[9] F. Tárkányi, S.M. Qaim, G. Stöcklin: Excitation functions of ^{3}He- and α-particle induced nuclear reactions on natural krypton: Production of ^{82}Sr at a compact cyclotron, Int. J. Appl. Radiat. Isotopes 39 (1988) 135

[10] F. Tárkányi, S.M. Qaim, G. Stöcklin: Excitation functions of ^{3}He-particle induced nuclear reactions on enriched ^{82}Kr and ^{83}Kr, Radiochimica Acta, in press

[11] S.M. Qaim, M.S. Sutisna, H. Ollig: Production of ^{38}K via the $^{35}Cl(\alpha,n)$-process at a compact cyclotron, Int. J. Appl. Radiat. Isotopes, in press

INSTITUT FÜR REAKTORENTWICKLUNG
KERNFORSCHUNGSANLAGE JÜLICH

1. Prediction of Double Differential (p,xn) - Cross Sections

P. Cloth, P. Dragovitsch and D. Filges

Studies of the neutron production from high-energy proton bombardment with an intranuclear cascade - evaporation model (INCE) were done for target nuclides Al-27, Zr-90 and Pb-208 at incident proton energies of 80, 160, 318 and 800 MeV to predict double differential cross sections for neutron emission. The intension was to create a comprehensive data base for comparison with other nuclear models on the one hand and for validation with experimental data on the other hand. The cross sections calculations were performed with the socalled thin target setup of the HETC/KFA-2 code of the HERMES system /1/. The INCE model is used without extra-nuclear transport. Therefore, the emitted neutrons are not able to undergo any further nuclear reaction with other nuclei. In all cases an isotropic emission for evaporation was assumed, the variable B_0-option was taken into account, and high energy fission was excluded. The number of calculated events for each problem was chosen to reach sufficient statistics although a high energy- and angle- resolution was demanded. A smooth and reliable shape also at medium

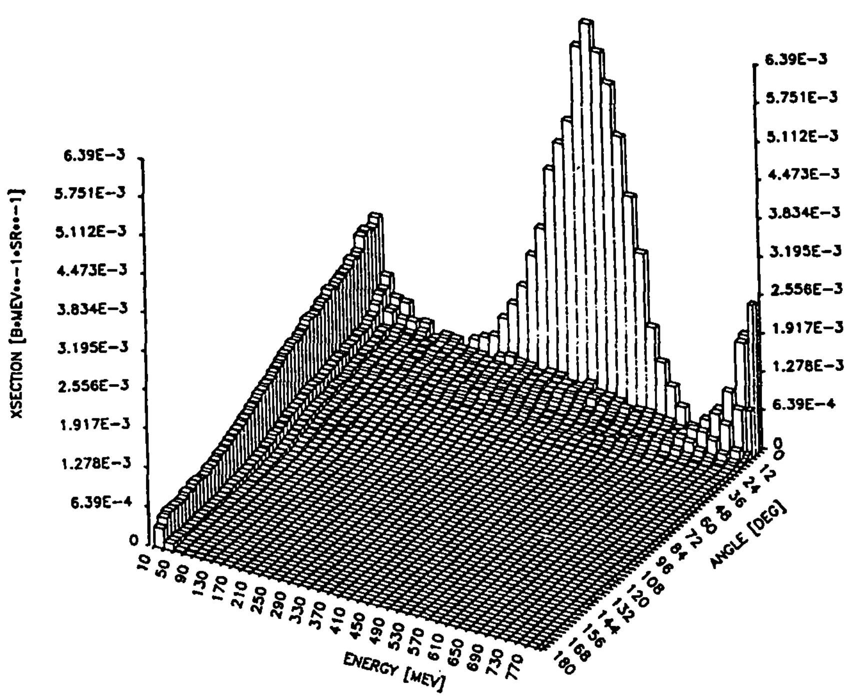

Fig. 1.-1.: Double differential cross sections for p-induced neutron emission at an incident proton energy of 800 MeV and for target nuclide Al-27.

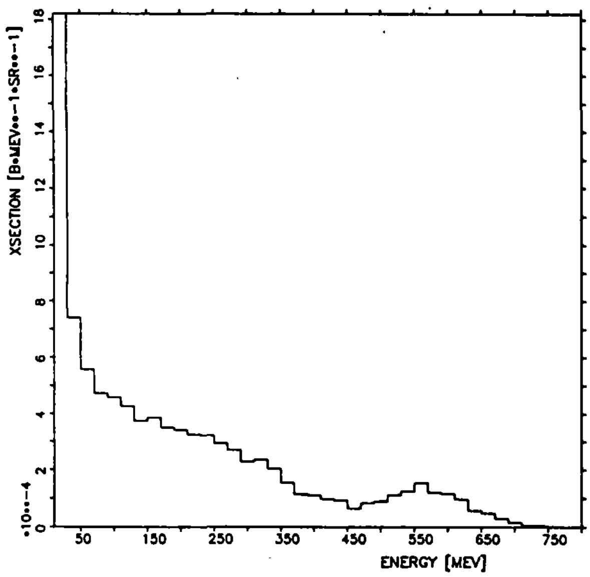

Fig. 1.-2.: Double differential cross sections for p-induced neutron emission under angles between 27 and 30 degree. Incident proton energy: 800 MeV; Target nuclide: Al-27.

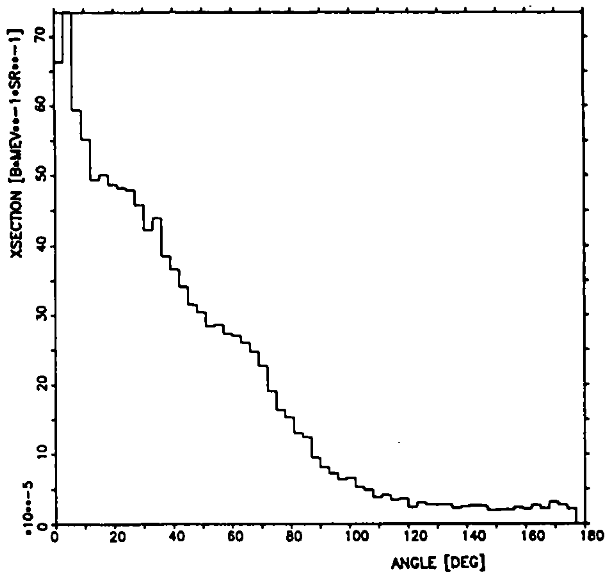

Fig. 1.-3.: Double differential cross sections for p-induced emission of neutrons with energies between 90 and 100 MeV. Incident proton energy: 800 MeV; Target nuclide: Al-27.

energies could be determined over the whole energy- and angle range (fig. 1.-1). The behaviour of the double differential cross sections can be ovserved in great detail for all neutron energies at discret angles (fig. 1.-2) and for angular distributions of emitted neutrons in discret energy groups (fig. 1.-3). The present results will be useful for a future fit of pre-equilibrium decay in the INCE model but also for validation with experimental data (see abstract no. 2).

2. Validation of (p,xn) Time-of-Flight Cross Section Measurements

W. Amian, P. Cloth, P. Dragovitsch, D. Filges and N. Paul

The recently measured and now evaluated time of flight measurements done at Los Alamos /2-4/ were compared with detailed HERMES calculations /1/ based on the intranuclear cascade - evaporation model. The calculational procedure is described in abstract no. 1. At 318 MeV incident proton energy and at small angles (fig. 2.-1) the calculations show a quite good agreement with the experiment in the range of evaporation and can also reproduce the quasi elastic peak at high energies in a fairly good manner. In the typical range of preequilibrium emission an underestimation can be observed. An excellent agreement is reached at proton energies of 800 MeV (Fig. 2.-2). In this case no significant influence of preequilibrium emission can be seen but slight discrepancies at the quasi elastic peak have to be remarked. The experimental data and their comparison with the INCE calculations will be discussed in a future publication.

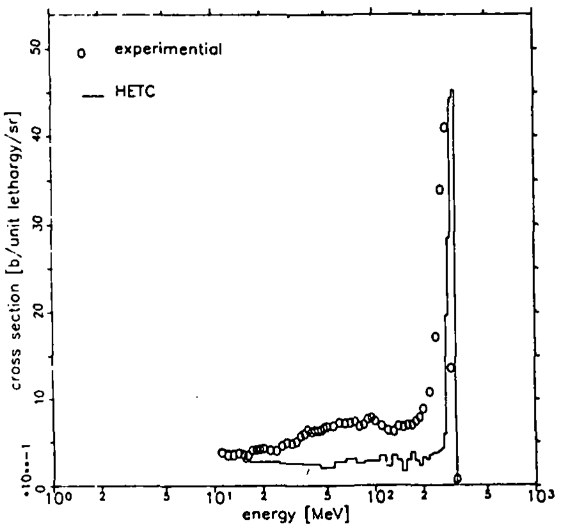

Fig. 2.-1.: Comparision of double differential (p,xn) cross section measured with ToF (experimental) with HETC/KFA-2 results (HETC). Incident proton energy: 318 MeV, Target nuclide: Pb-208, n-emission under 7.5 degree.

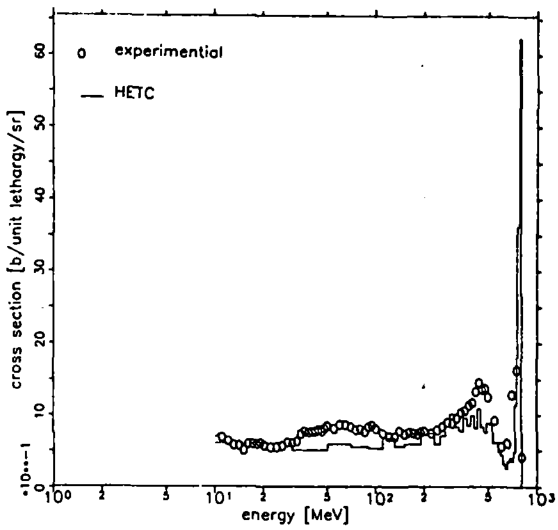

Fig. 2.-2.: Comparision of double differential (p,xn) cross section measured with ToF (experimental) with HETC/KFA-2 results (HETC). Incident proton energy: 800 MeV, Target nuclide: Pb-208, n-emission under 7.5 degree.

References:

/1/ P.Cloth et al.: HERMES, High Energy Radiation Monte Carlo Elaborate System, KFA-Report, in print.

/2/ M.M. Meier, W.B. Amian et al.: 318 and 800 MeV (p,xn) Cross Sections
Proc. of Int. Conf., Santa Fe, USA, May 1985

/3/ W.Amian et al., Special Report NEANDC(E)-282 U Vol.V INDC(Ger)-30/LN+Special

/4/ M.M. Meier et al., to be published in Phys.Rev. C

ZENTRALEINRICHTUNG FÜR STRAHLENSCHUTZ
UNIVERSITÄT HANNOVER

1. Measurement and Theoretical Interpretation of Thin-Target Cross Sections and Thick-Target Production Rates

R. Michel, P. Dragovitsch[1], K. Prescher[2], M.N. Rao[3], J. Methew[3]

1.1 Depth profiles of production Rates in Artificial Meteoroids with Radii between 5 and 25 cm Isotropically Irradiated with 600 MeV Protons

In the course of the experiment CERN SC96 (Cologne Collaboration) three artificial meteoroids made out of diorite and gabbro were isotropically irradiated with 600 MeV protons in order to simulate the production in meteoroids of cosmogenic nuclides by galactic cosmic ray protons. The artificial meteoroids, having a density of 3 g cm^{-3} covered radii of 5, 15 and 25 cm. The depth dependent production of a wide range of radionuclides from target elements O, Mg, Al, Si, Ti, Fe, Co, Ni, Cu, Ba, Lu, and Au was measured. Furthermore, the production of He and Ne isotopes from Mg, Al, and Si as well from degassed meteoritic material was determined. The observed depth profiles show a wide variety of shapes (Fig. 1). Low energy products have pronounced maxima in the center, high energy products exhibit strong decreases from surface to center and, in between, essentially flat profiles are seen as well as such with transition maxima. The center production rates in the three artificial meteoroids (Fig. 2) give an impression about the size dependences of production rates. Low energy products increase by up to a factor of 3.5, while for extreme high energy products the center production rates decrease up to a factor of 10.

Using Monte Carlo techniques the spectra of primary protons and of secondary protons and neutrons in the artificial meteoroids were calculated. On the basis of these spectra and of thin-target excitation functions, theoretical depth profiles were calculated and compared with the experimental data. Figs. 3 and 4 give exemplarily the depth profiles for the production of ^{59}Fe and ^{57}Ni from Co. The production of the first one of these nuclides is exclusively due to neutron-induced reactions, while the second one only is produced by protons. A

1 IRE/KFA Juelich. 2 Interatom/Bergisch-Gladbach. 3 PRL/Ahmedabad

comprehensive survey on all the results obtained so far is published elsewhere [1,2]. The excellent agreement between theory and experiment demonstrates the quality of the theoretical approach. The theoretical depth profiles allow to distinguish the different contributions of primary and secondary particles and to unravel the various production modes of cosmogenic nuclides in meteoroids. This analysis shows that it is possible to model the production of residual nuclides in artificial meteoroids with excellent accuracy by thin-target calculations, provided that reliable thin-target excitation functions are at hand.

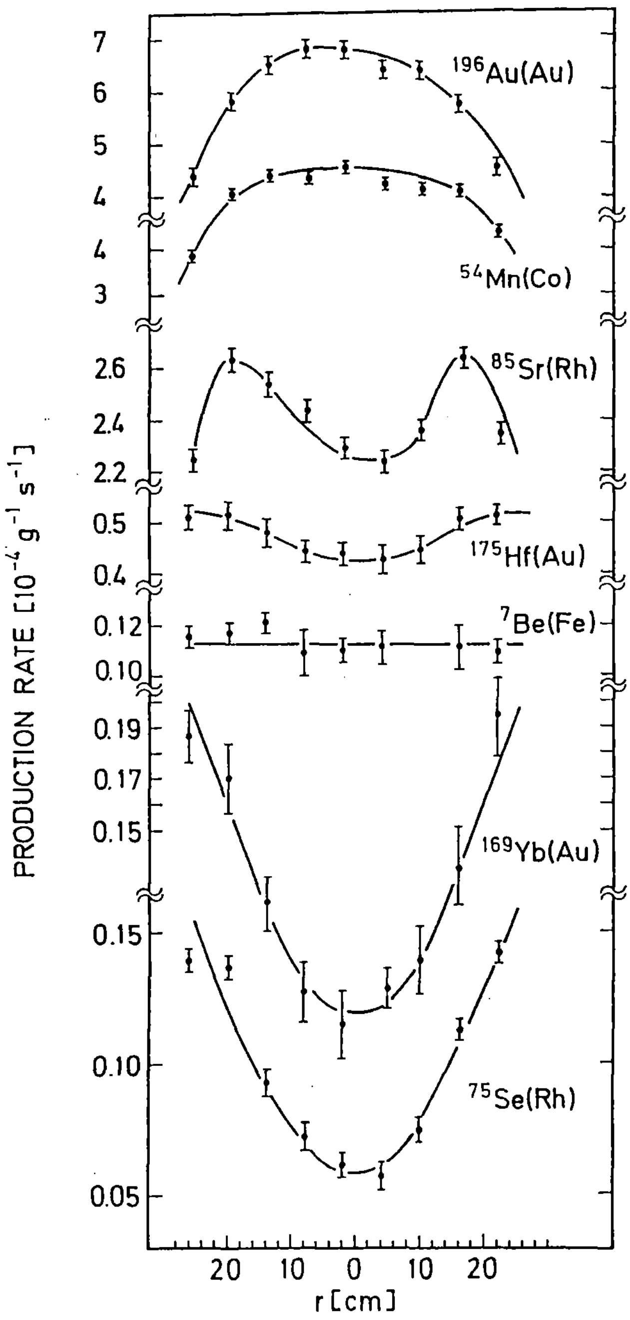

Fig. 1 Depth profiles of the production of radionuclides as measured in an artificial meteoroid with a radius of 25 cm irradiated isotropically with 600 MeV protons. The data are normalized to a primary p-flux of 1 cm^{-2} s^{-1}.

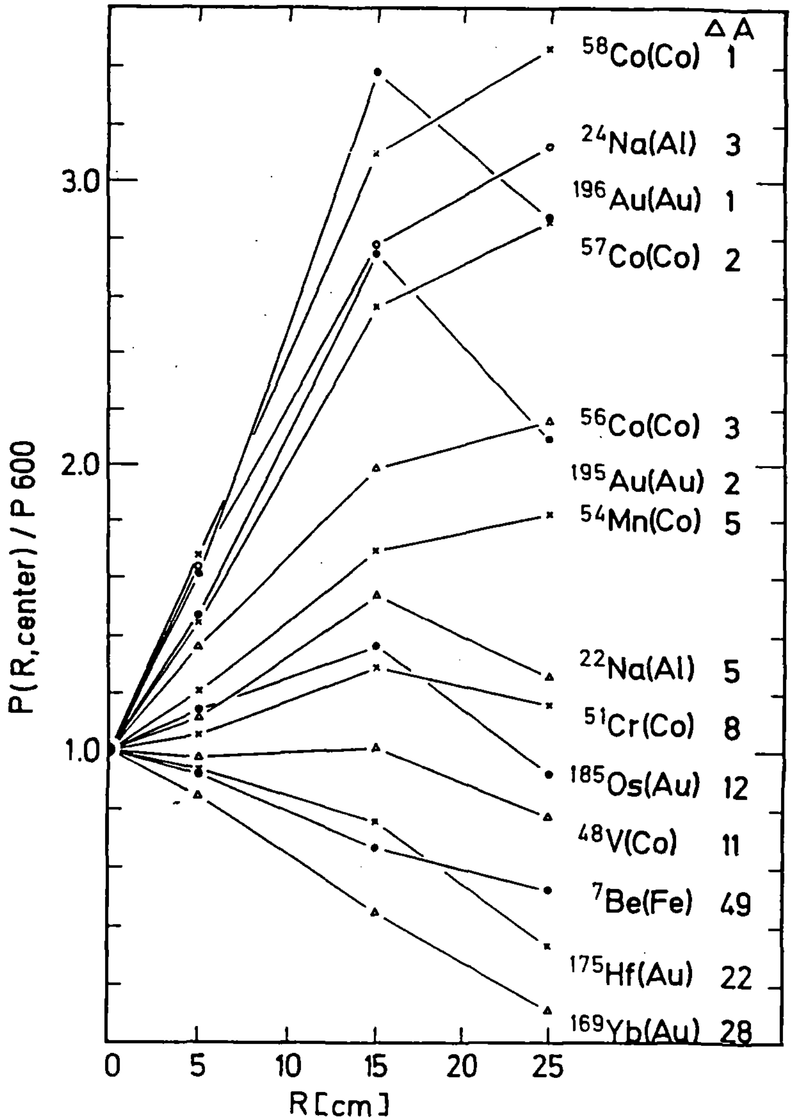

Fig. 2 Experimental production rates in the centers of artificial meteoroids normalized to the 600 MeV thin-target production rates as a function of radius of the artificial meteoroid.

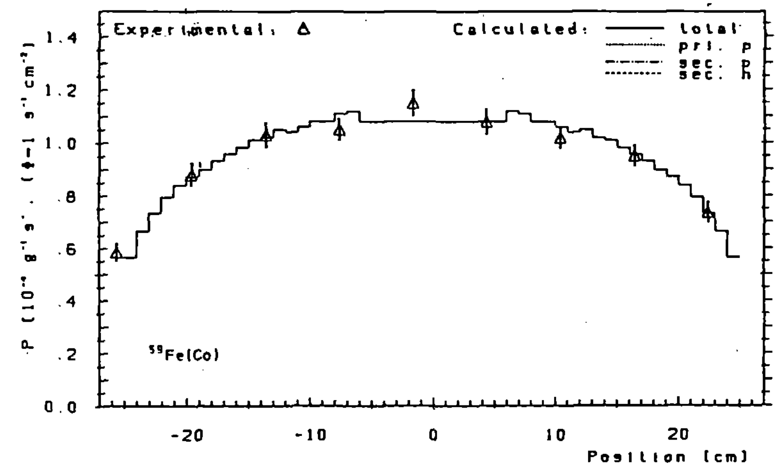

Fig. 3 Comparison of experimental and theoretical production rates of ^{59}Fe from Co in an artificial meteoroid with radius of 25 cm. This reaction is exclusively due to secondary neutrons.

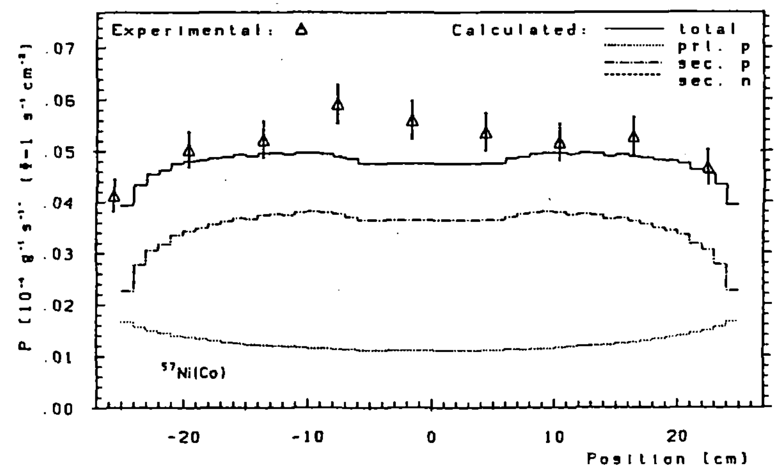

Fig. 4 Comparison of experimental and theoretical production rates of ^{57}Ni from Co in an artificial meteoroid with radius of 25 cm. This reaction is exclusively due to primary and secondary protons.

1.2 Production of Radionuclides by Proton-Induced Spallation at 600 MeV

In the course of a research programm to investigate the transition from preequilibrium to spallation reactions, done in collaboration of groups from Cologne, Hannover, and Zürich, thin-target cross sections for the production of radionuclides by proton-induced reactions on O, Mg, Al, Si, Ti, V, Cr, Mn, Fe, Co, Ni, Cu, Y, and Zr were measured at 600 MeV. Data on the target elements Rh, Ba, and Au are about to be finalized. The experiments were extended to p-energies of 1200 and 2600 MeV. These mesurements are not yet finished. Further irradiations at 800 MeV and between 50 and 200 MeV are in preparation.

The existing data (Table I) already allow for a comprehensive survey on the quality of the often used semi-empirical formulas for the calculation of cross sections for the production of residual nuclei by high-energy reactions. Table I also gives the results of calculations by Rudstam's CDMDG and CDMD formulas [3] and by the formula by Silberberg and Tsao [4]. The calculations were done by the code SPALL by Routti and Sandberg [5]. A comparison of theoretical and experimental data shows partially severe discrepancies. Tough considerable improvements have been achieved in the more recent formula [4], in particular with respect to the production of light fragments, for many nuclides theory and experiment deviate by more than a factor of two. The calculational accuracy obtained so far is not sufficient for the application of these formulas in astrophysics and cosmochemistry. Therefore, presently the capabilities of Monte Carlo calculations in the form of the code HETC [6] for the a priori calculation of integral production cross sections are tested.

1.3 Thin-Target Excitation Functions for the Production of Xenon-Isotopes from Barium

Thin-target excitation functions for the proton-induced production of radionuclides [7] and stable Xe isotopes (table II) from barium were measured at the JULIC cyclotron of the IKP/KFA Juelich up to E_p = 45 MeV using the stacked-foil technique. For stable Xe-isotopes the new thin-target data are not compatible with earlier measurements by Kaiser [8] who investigated the p-energy range from 35 to 600 MeV. Because of the narrow overlap in energy between the two investigations, presently the measurements are extended to higher energies and

Table I Experimental Thin-Target Cross Sections for the Production of Radionuclides by 600 MeV Protons. * monitor cross section.

Reaction	Cross section [mb] experimental this work	calculated CDMDG	calculated CDMD	[4]
O(P,5PXN)BE- 7	11.3 ± 0.5	1.69	1.55	7.91
MG(P,9PXN)BE- 7	6.43 ± 0.28	0.514	0.522	3.79
MG(P,2PXN)NA- 22	31.5 ± 1.3	20.4	18.3	20.3
MG(P,2PXN)NA- 24	7.94 ± 0.38	30.9	29.2	9.66
AL(P,10P11N)BE- 7	4.88 + 0.10	0.35	0.367	2.83
AL(P,3P3N)NA- 22	16.00*	13.9	12.9	14.1
AL(P,3PN)NA- 24	11.3 ± 0.3	21.1	20.6	9.53
SI(P,11PXN)BE- 7	5.39 ± 0.22	0.299	0.318	2.84
SI(P,4PXN)NA- 22	19.6 ± 0.6	11.9	11.2	14.8
SI(P,4PXN)NA- 24	5.15 ± 0.19	18.0	17.8	0.578
TI(P,19P,XN)BE- 7	1.95 ± 0.09	0.018	0.017	1.72
TI(P,12PXN)NA- 22	0.90 ± 0.04	0.696	0.837	0.989
TI(P,12PXN)NA- 24	1.37 ± 0.09	1.06	1.33	1.42
TI(P,4PXN) K- 42	9.01 ± 0.48	12.4	10.5	6.37
TI(P,4PXN) K- 43	3.68 ± 0.24	3.8	2.9	2.1
TI(P,3PXN)CA- 47	0.26 ± 0.01	0.19	0.24	0.163
TI(P,2PXN)SC- 46	32.0 ± 1.2	37.0	33.7	19.4
TI(P,2PXN)SC- 47	28.4 ± 1.1	15.3	10.9	7.88
TI(P,2PXN)SC- 48	2.97 ± 0.14	3.77	2.76	1.73
TI(P,XN) V- 48	1.90 ± 0.08	46.9	44.5	39.7
V(P,20PXN)BE- 7	1.72 ± 0.08	0.013	0.018	1.73
V(P,13PXN)NA- 22	0.56 ± 0.03	0.513	0.633	0.763
V(P,13PXN)NA- 24	1.10 ± 0.06	0.778	1.01	1.05
V(P,5PXN) K- 43	2.46 ± 0.15	2.28	2.19	1.42
V(P,4PXN)CA- 47	0.36 ± 0.04	0.140	0.182	0.102
V(P,3PXN)SC- 46	23.3 ± 0.9	26.3	24.5	13.8
V(P,3PXN)SC- 47	15.4 ± 0.9	11.3	8.27	5.36
V(P,3PXN)SC- 48	4.88 ± 0.21	2.78	2.09	1.13
V(P,PXN) V- 48	13.4 ± 3.4	34.5	33.7	33.1
V(P,XN)CR- 48	0.047± 0.002	1.52	1.45	2.07
V(P,XN)CR- 51	2.58 ± 0.11	82.6	100.	95.2

Table I (continued)

Reaction	Cross section [mb] experimental this work	calculated CDMDG	calculated CDMD	[4]
CR(P,14PXN)NA- 22	2.48 ± 0.20	0.382	0.483	0.607
CR(P,6PXN) K- 43	6.18 ± 0.59	2.09	1.67	0.982
CR(P,5PXN)CA- 47	0.22 ± 0.03	0.104	0.139	0.069
CR(P,4PXN)SC- 46	48.1 ± 2.8	19.6	18.7	9.77
CR(P,4PXN)SC- 47	20.0 ± 1.1	8.41	6.32	3.73
CR(P,4PXN)SC- 48	3.60 ± 0.22	2.07	1.59	0.773
CR(P,2PXN) V- 48	77.4 ± 4.3	25.7	25.7	26.0
CR(P,PXN)CR- 48	2.11 ± 0.13	1.13	1.11	1.91
CR(P,PXN)CR- 51	180.0 ± 9.9	61.6	76.6	71.7
CR(P,XN)MN- 52	1.38 ± 0.12	33.1	28.8	30.4
MN(P,22P27N)BE- 7	1.68 ± 0.12	0.006	0.009	1.540
MN(P,15P19N)NA- 22	3.82 ± 0.20	0.249	0.326	0.381
MN(P,5P5N)SC- 46	14.00 ± 0.52	12.7	12.6	7.82
MN(P,3P5N) V- 48	15.7 ± 0.8	16.7	17.4	14.8
MN(P,2P6N)CR- 48	0.10 ± 0.08	0.737	0.750	0.926
MN(P,2P3N)CR- 51	41.70 ± 1.64	40.0	51.7	47.0
MN(P,P3N)MN- 52	6.21 ± 0.25	21.5	19.4	16.4
MN(P,PN)MN- 54	61.0 ± 2.3	68.3	87.3	76.6
FE(P,23PXN)BE- 7	2.01 ± 0.09	0.005	0.008	1.79
FE(P,16PXN)NA- 22	0.40 ± 0.03	0.218	0.290	0.396
FE(P,8PXN) K- 43	0.95 ± 0.05	1.19	1.00	0.437
FE(P,6PXN)SC- 46	9.44 ± 0.37	11.2	11.2	4.73
FE(P,6PXN)SC- 47	2.89 ± 0.11	4.80	3.79	1.67
FE(P,4PXN) V- 48	22.7 ± 0.80	14.7	15.4	18.7
FE(P,3PXN)CR- 48	0.62 ± 0.12	0.647	0.666	1.57
FE(P,3PXN)CR- 51	46.3 ± 1.7	35.2	46.0	49.0
FE(P,2PXN)MN- 52	11.5 ± 0.6	18.9	17.2	22.8
FE(P,2PXN)MN- 54	39.8 ± 1.5	60.0	77.5	52.9
FE(P,XN)CO- 56	1.36 ± 0.06	21.5	17.9	25.8
FE(P,XN)CO- 57	0.23 ± 0.01	63.7	63.0	91.5
CO(P,26P27N)BE- 7	1.61 ± 0.07	0.004	0.005	1.59
CO(P,17P21N)NA- 22	0.18 ± 0.02	0.139	0.192	0.308
CO(P,9P8N) K- 43	1.06 ± 0.05	0.758	0.664	0.380

Table I (continued)

Reaction	Cross section [mb] experimental this work	calculated CDMDG	calculated CDMD	[4]
CO(P,7P7N)SC- 46	8.86 ± 0.34	7.120	7.41	3.84
CO(P,7P6N)SC- 47	3.34 ± 0.13	3.06	2.51	1.44
CO(P,7P5N)SC- 48	0.93 ± 0.07	0.752	0.632	0.296
CO(P,5P7N) V- 48	16.10 ± 0.85	9.35	10.2	10.4
CO(P,4P8N)CR- 48	0.37 ± 0.02	0.412	0.441	0.737
CO(P,4P5N)CR- 51	37.9 ± 1.5	22.4	30.4	30.7
CO(P,3P5N)MN- 52	11.2 ± 0.5	12.0	11.4	12.0
CO(P,3P3N)MN- 54	30.8 ± 1.2	38.2	51.3	40.5
CO(P,P4N)CO- 55	0.87 ± 0.11	2.67	2.45	3.3
CO(P,P3N)CO- 56	8.97 ± 0.35	13.7	11.8	12.9
CO(P,P2N)CO- 57	28.3 ± 1.1	40.6	41.7	50.5
CO(P,PN)CO- 58	59.8 ± 2.4	71.4	96.4	88.3
CO(P,3N)NI- 57	0.22 ± 0.02	2.45	2.24	2.87
NI(P,25PXN)BE- 7	2.63 ± 0.12	0.004	0.006	1.98
NI(P,18PXN)NA- 22	0.39 ± 0.03	0.146	0.200	0.393
NI(P,8PXN)SC- 46	5.03 ± 0.19	7.47	7.74	1.98
NI(P,6PXN) V- 48	22.7 ± 0.9	9.81	10.6	17.9
NI(P,5PXN)CR- 48	1.86 ± 0.10	0.433	0.46	2.24
NI(P,5PXN)CR- 51	42.8 ± 1.6	23.5	31.7	29.4
NI(P,4PXN)MN- 52	15.8 ± 0.6	12.6	11.9	24.7
NI(P,4PXN)MN- 54	16.4 ± 0.7	40.1	53.6	24.2
NI(P,3PXN)FE- 59	0.30 ± 0.02	10.1	6.37	1.47
NI(P,2PXN)CO- 56	38.4 ± 1.5	14.3	12.3	31.3
NI(P,2PXN)CO- 57	75.6 ± 2.8	42.6	43.6	85.8
NI(P,2PXN)CO- 58	23.4 ± 0.9	74.9	101.	62.6
NI(P,2PXN)CO- 60	2.31 ± 0.22	52.2	38.0	10.4
NI(P,PXN)NI- 56	2.25 ± 0.19	0.261	0.374	2.54
NI(P,PXN)NI- 57	23.7 ± 0.9	2.57	2.43	9.50
CU(P,26PXN)BE- 7	1.61 ± 0.08	0.002	0.003	0.619
CU(P,19PXN)NA- 22	0.14 ± 0.02	0.072	0.104	0.297
CU(P,11PXN) K- 43	0.51 ± 0.03	0.390	0.361	0.287
CU(P,9PXN)SC- 46	5.50 ± 0.21	3.66	4.04	2.89
CU(P,9PXN)SC- 47	2.33 ± 0.09	1.57	1.36	1.09

Table I (continued)

Reaction	Cross section [mb] experimental this work	calculated CDMDG	calculated CDMD	[4]
CU(P,7PXN) V- 48	11.1 ± 0.4	4.81	5.55	5.70
CU(P,6PXN)CR- 51	27.7 ± 1.0	11.5	16.5	16.2
CU(P,5PXN)MN- 52	9.35 ± 0.35	6.19	6.21	6.78
CU(P,5PXN)MN- 54	23.1 ± 0.9	19.7	27.9	20.9
CU(P,4PXN)FE- 59	1.70 ± 0.20	4.97	3.32	2.24
CU(P,3PXN)CO- 56	10.3 ± 0.4	7.03	6.43	7.77
CU(P,3PXN)CO- 57	27.7 ± 1.0	20.9	22.7	29.2
CU(P,3PXN)CO- 58	34.4 ± 1.4	36.7	52.5	45.3
CU(P,3PXN)CO- 60	11.9 ± 0.5	25.6	19.8	13.3
CU(P,2PXN)NI- 57	1.00 ± 0.04	1.26	1.27	1.8
Y(P,XPYN)BE- 7	1.95 ± 0.20	0.0004	0.001	0.328
Y(P,10P15N)ZN- 65	8.20 ± 0.50	2.72	5.04	4.69
Y(P,9P14N)GA- 67	12.2 ± 0.7	3.57	6.15	6.34
Y(P,8P13N)GE- 69	11.5 ± 0.6	4.48	7.04	6.53
Y(P,7P9N)AS- 74	7.58 ± 0.36	5.68	4.59	3.84
Y(P,6P9N)SE- 75	34.9 ± 1.3	12.70	16.20	14.40
Y(P,3P4N)RB- 83	67.5 ± 3.5	32.8	26.1	27.3
Y(P,3P3N)RB- 84	16.3 ± 0.7	19.4	11.4	10.2
Y(P,2P3N)SR- 85	57.0 ± 3.7	53.8	47.7	44.8
Y(P,P2N) Y- 87	60.9 ± 2.3	83.1	83.6	87.2
Y(P,PN) Y- 88	88.3 ± 3.4	66.0	44.8	39.8
ZR(P,11PXN)ZN- 65	5.22 ± 0.57	1.99	3.77	3.23
ZR(P,10PXN)GA- 67	7.51 ± 0.35	2.61	4.60	4.84
ZR(P,7PXN)SE- 75	28.0 ± 1.1	9.26	12.20	9.64
ZR(P,4PXN)RB- 83	55.2 ± 2.9	24.0	19.6	18.4
ZR(P,4PXN)RB- 84	9.50 ± 0.40	14.200	8.54	7.02
ZR(P,3PXN)SR- 85	102.0 ± 9.7	39.3	35.7	30.3
ZR(P,2PXN) Y- 87	66.9 ± 2.5	60.8	62.6	58.2
ZR(P,2PXN) Y- 88	51.1 ± 2.7	48.3	35.5	27.3
ZR(P,2PXN) Y- 91	19.4 ± 1.5	34.2	16.2	17.5
ZR(P,PXN)ZR- 88	44.8 ± 2.4	69.1	97.2	
ZR(P,PXN)ZR- 89	58.6 ± 2.2	88.7	105.0	85.5
ZR(P,PXN)ZR- 95	2.42 + 0.15	0.466	0.307	0.326

Table II Cross Sections for the Production of Xe form Ba

Energy [MeV]	Cross Section [mb] ^{126}Xe	^{128}Xe	^{129}Xe	^{130}Xe	^{131}Xe	^{132}Xe	^{134}Xe
11.90		9.50E-04	5.15E-04	7.99E-04	2.50E-02	4.18E-02	
±0.78		±1.43E-04	±7.73E-05	±1.20E-04	±3.76E-03	±6.28E-03	
18.21			7.36E-01	2.57E-03	1.27E+00	2.50E-01	
±0.58			±1.71E-01	±5.95E-04	±2.55E-01	±4.99E-02	
20.06	9.49E-04	2.38E-03	8.19E-01	1.35E-02	1.13E+00	2.31E-01	
±0.52	±1.44E-04	±3.61E-04	±1.23E-01	±2.04E-03	±1.71E-01	±3.47E-02	
22.02	6.27E-03	7.42E-03	1.33E+00	6.79E-02	1.80E+00	4.12E-01	
±0.52	±1.26E-03	±1.52E-03	±2.66E-01	±1.36E-02	±3.60E-01	±8.24E-02	
26.38	1.35E-02	2.16E-02	1.04E+00	1.29E-01	1.52E+00	4.66E-01	1.87E-04
±0.88	±2.03E-03	±3.25E-03	±1.56E-01	±1.94E-02	±2.28E-01	±7.00E-02	±2.80E-05
27.68	2.96E-02	1.22E-01	1.46E+00	3.20E-01	2.11E+00	8.64E-01	
±0.68	±5.95E-03	±2.44E-02	±2.93E-01	±6.42E-02	±4.23E-01	±1.73E-01	
31.81	3.22E-02	6.80E-01	8.81E-01	6.93E-01	1.58E+00	1.19E+00	2.62E-02
±0.57	±6.48E-03	±1.36E-01	±1.76E-01	±1.39E-01	±3.17E-01	±2.37E-01	±5.85E-03
32.22	2.76E-02	5.08E-01	7.96E-01	5.31E-01	1.36E+00	9.72E-01	2.60E-02
±0.72	±4.17E-03	±7.67E-02	±1.20E-01	±8.01E-02	±2.89E-01	±1.46E-01	±3.92E-03
33.98	3.18E-02	1.03E+00	9.06E-01	1.06E+00	2.85E+00	1.65E+00	5.40E-02
±0.50	±6.37E-03	±2.06E-01	±1.81E-01	±2.13E-01	±5.70E-01	±3.29E-01	±1.13E-02
36.42	1.64E-02	7.18E-01	6.20E-01	8.06E-01	3.59E+00	1.22E+00	5.62E-02
±0.64	±2.47E-03	±1.08E-01	±9.35E-02	±1.22E-01	±7.61E-01	±1.84E-01	±8.47E-03
37.72	1.66E-02	9.72E-01	1.06E+00	1.22E+00	9.98E+00	2.10E+00	8.58E-02
±0.64	±3.43E-03	±1.95E-01	±2.12E-01	±2.45E-01	±2.00E+00	±4.21E-01	±1.73E-02
39.96	1.69E-02	1.08E+00	1.76E+00	1.52E+00	1.66E+01	3.75E+00	1.41E-01
±0.58	±3.40E-03	±2.17E-01	±3.52E-01	±3.05E-01	±3.33E+00	±7.51E-01	±2.82E-02
40.59	1.40E-02	9.45E-01	1.41E+00	1.31E+00	1.41E+01	3.04E+00	1.06E-01
±0.55	±2.12E-03	±1.42E-01	±2.12E-01	±1.98E-01	±2.13E+00	±4.56E-01	±1.59E-02
44.17	3.04E-02	1.12E+00	2.81E+00	2.04E+00	2.88E+01	8.00E+00	1.57E-01
±0.45	±1.01E-03	±2.81E-02	±7.14E-02	±5.19E-02	±7.27E-01	±1.60E-01	±4.48E-03

a detailed theoretical analysis using the code ALICE LIVERMORE 87 [9] is performed. After unravelling the existing discrepancies, the data shall provide a basis for the interpretation of Xe production depth profiles measured in terrestrial simulation experiments and in lunar and meteoritical materials.

References

[1] D. Aylmer, F. Begemann, P. Cloth, P. Dragovitsch, P. Englert, D. Filges, U. Herpers, G.F. Herzog, A. Jermaikan, J. Klein, T.H. Kruse, R. Michel, R.K. Moniot, R. Middleton, F. Peiffer, P. Signer, R. Stück, S. Theis, C. Tuniz, S. Vadja, H. Weber, R. Wieler, Jül-2130 (1987).

[2] R. Michel, F. Peiffer, S. Theis, F. Begemann, H. Weber, P. Signer, R. Wieler, P. Cloth, P. Dragovitsch, D. Filges, P. Englert, Nucl. Instr. Meth. Phys. Res. B, to be submitted (1988).

[3] G. Rudstam, Z. Naturf. 21a (1966) 1027.

[4] R. Silberberg, C.H. Tsao, Astrophys. J. Suppl. 25 (1973) 315.

[5] J.T. Routti, J.V. Sandberg, Comp. Phys. Comm. 23 (1981) 411.

[6] P. Cloth, D. Filges, G. Sterzenbach, T.W. Armstrong, B.L. Colburn, Jül-Spez-196 (1983).

[7] F. Peiffer, Thesis, University Cologne (1986).

[8] W.A. Kaiser, Phil. Trans. Royal Soc. London A 285 (1977) 337.

[9] M. Blann, priv. comm. (1987).

This work was partially supported by the Deutsche Forechungsgemeinschaft and by BMFT/DFVLR-ISRO.

ABTEILUNG NUKLEARCHEMIE
UNIVERSITÄT ZU KÖLN

Cross Sections and Production Rates for Application in Cosmochemistry

B. Dittrich, U. Herpers, Th. Schiffmann

1. Thin-Target Excitation Functions for Proton-Produced Long-Lived Radionuclides

In the course of a research progamm to investigate the transition from preequilibrium to spallation reactions, done in collaboration of groups from Cologne, Hannover and Zürich, thin-target cross sections for the production of radionuclides by proton-induced reactions on various elements were measured at 600 MeV. The experiments were extended to p-energies of 1200 and 2600 MeV, the measurements still being not finished. Further irradiations at 800 MeV and between 50 and 200 MeV are in preparation.

Here we want to report our results of the determination of cross sections of spallation reactions using 600 MeV protons from the target materials titanium, iron, cobalt and nickel and for titanium targets for lower energies, additionally.

The radionuclides Na-22, Ti-44, Mn-54 and Co-57 were measured by gamma-spectrometry. To determine the cross sections of the reaction Ti(p,19pxn)Be-10, we had to separate several products in a chemical analysis followed by Accelerator Mass Spectrometry (AMS). The cross sections determined are given in table 1.

The experimental results partly were compared with the theoretical calculations by the program SPALL from Routti and Sandberg [1] which is based on the model of Silberberg and Tsao [2]. For a detailed description of the calculation see Ref. [3 and 4]. It was found that the modell of Silberberg and Tsao [2] is usable for spallation only whereas a large difference between experiment and theory is found for small mass-differences between target and product.

Table 1: Experimental and theoretical thin target cross sections for p-induced reactions

Reaction	Energy [MeV]	Cross section [mb] experimental	Cross section [mb] calculated
Ti(p,19pxn)Be-10	118	0.057 ± 0.004	
	168	0.092 ± 0.006	
	196	0.116 ± 0.007	
	600	0.845 ± 0.048	
Ti(p,12pxn)Na-22	600	0.991 ± 0.079	0.989
Ti(p,pxn)Ti-44	91	2.760 ± 0.180	
	109	2.670 ± 0.180	
	126	2.370 ± 0.160	
	135	2.250 ± 0.150	
	150	2.120 ± 0.150	
	162	2.060 ± 0.140	
	174	2.010 ± 0.140	
	185	1.820 ± 0.120	
	196	1.770 ± 0.120	
	600	1.330 ± 0.100	
Fe(p,16pxn)Na-22	600	0.420 ± 0.020	0.396
Fe(p,2pxn)Mn-54		48.480 ± 1.800	52.9
Fe(p,xn)Co-57		0.250 ± 0.010	91.5
Co(p,17p21n)Na-22	600	0.260 ± 0.010	0.308
Co(p,3p3n)Mn-54		36.810 ± 1.250	40.5
Ni(p,18pxn)Na-22	600	0.390 ± 0.020	0.393
Ni(p,4pxn)Mn-54		18.210 ± 0.660	24.2
Ni(p,2pxn)Co-60		1.830 ± 0.070	10.4

2. Production Rates and Depth Profiles of Cosmochemical Relevant Radionuclides from Simulation Experiments

In the last edition of the NEANDC-Report P. Dragovitsch et al. [5] reported about the simulation experiments with artificial meteoroides with radii of 5, 15 and 25 cm isotropically irradiated with 600 MeV protons at CERN synchrocyclotron. After measuring the short-lived nuclides [3 and 4] we started the determination of production rates of long-lived radionuclides. This work was performed by long-term measurements of Na-22, Ti-44, Mn-54 and Co-57 by gamma-spectrometry and Be-10 by accelerator mass spectrometry (AMS).

Thus it was possible to obtain the production rate data of the reactions leading from titanium to Be-10, Na-22 and Ti-44, from iron to Be-10, Na-22 and Co-57 and from cobalt and nickel to Na-22 from all targets of the simulation experiments. Several production rates and depth profiles from the target material for short-lived radionuclides have allready been published [6]. Exemplary experimental and theoretical production rates depth-profiles are given in Fig. 1. Further results will be published elsewhere [7]

The experimental values were compared with the results of high-energy transport calculation by the HET/KFA Code [8] and the low-energy transport of neutrons by MORSE-Code [9], which are based on Monte Carlo techniques. The theoretical results were derived from the depth dependence of primary and secondary protons and secondary neutrons calculated by the code ALICE LIVERMORE [10] on the basis of the excitation functions for p-induced reactions.

The comparison of the theoretical with the experimental depth profiles shows some deviation ranging from 5% (see Fig. 1a) up to 30%, especially in reactions with a small mass difference between target and product.(see Fig. 1b). The latter is typical for all low energy reactions.

The high discrepancy is understandable because the calculation by the code ALICE LIVERMORE does not take into account the fragmentation of nuclides, high energy secondary particles and particles with extremly low energies.

Based on these experimental results it will be possible to discuss and to verify the models of high-energy nuclear reactions and high-energy transport. Until a detailed modell of low-energy processes is available there is a need for more accurate data for nuclear reactions at several energies.

Acknowledgement: We want to thank Prof. W. Wölfli and his coworkers of the ETH Zürich for the Be-10-measurement by AMS. This work was partially supported by the Deutsche Forschungsgemeinschaft.

References:

[1] J.T. Routti, J.V. Sandberg
Computer Physics Communication 23 (1981) 411

[2] R. Silberberg, C.H. Tsao,
Astrophys. J. Suppl 25 (1973) 315 and 335

[3] F. Peiffer, Thesis, Köln 1986

[4] P. Dragovitsch, Thesis, Köln 1987

[5] NEANDC (E)-282 U Vol. V/ INDC (Ger)-30/LN+Special

[6] Cologne Collaboration, Jül-Spez-2130 (1987)

[7] B. Dittrich et al.
Proceedings of the 2nd Internat. Conf. on Nuclear and Radiochemistry, Brighton 1988, in preparation

[8] P. Cloth et al.,Jül-Spez-196 (1983)

[9] M.B. Emmett, ORNL-4972 (1972)

[10] M. Blann, J. Bisplinghoff, UCID-19614 (1982)

a)

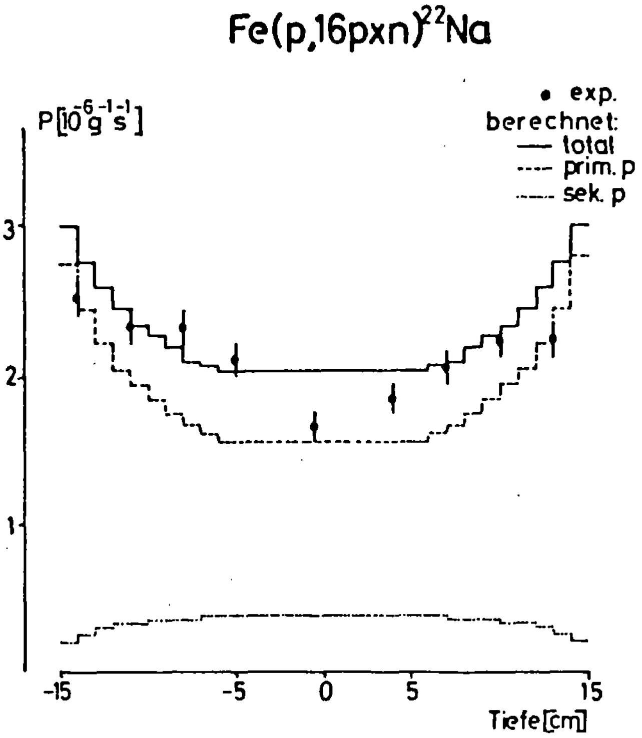

b)

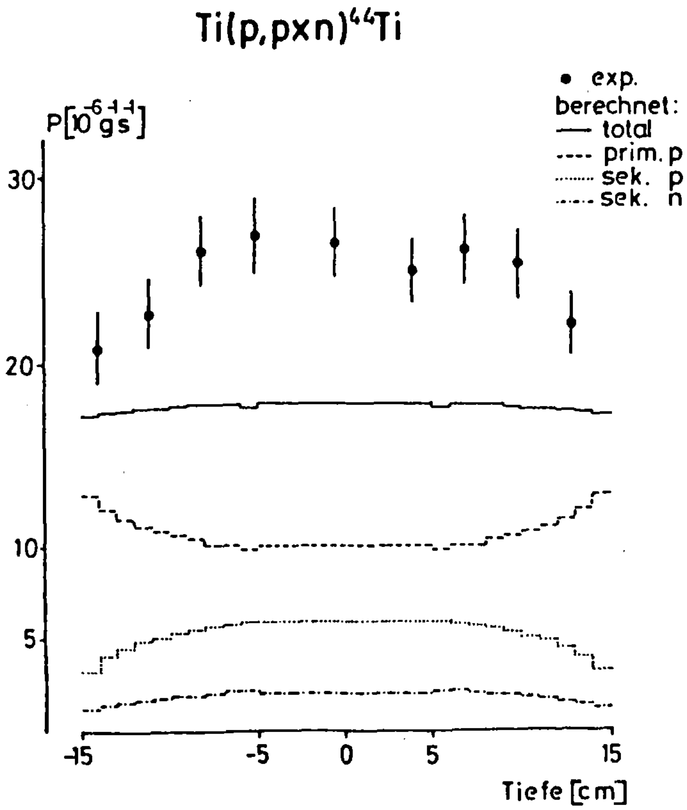

Fig.1 : Experimental and theoretical production depth profiles of Na-22 from Fe (Fig. 1a) and of Ti-44 from Ti (Fig. 1b) in the artifical meteoroid with 15 cm radius.

INSTITUT FÜR KERNCHEMIE
UNIVERSITÄT MAINZ

Nuclear Charge Distribution in the Reactor Neutron Induced Fission of ^{232}Th : Fractional Cumulative Yields of the Isotopes of Krypton and Xenon.

Alok Srivastava* and H. O. Denschlag

The fractional cumulative yields of several krypton and xenon isotopes in the reactor neutron induced fission of ^{232}Th were determined radiochemically using a continuous chemical separation of these rare gases from the remaining fission products by diffusion through a layer of Mg-stearate into a closed evacuated volume lined with filter paper. The irradiations were carried out in the central position of the Mainz TRIGA Reactor. After the end of irradiation appropriate descendents were isolated chemically from both the filter paper and stearate fractions, counted by γ-ray spectroscopy and the respective fractional cumulative yields of the rare gases were calculated.

The results are given in Table 1 and may be compared there to the literature values, as far as available.

It is observed that the values from the present work agree well with those obtained by Izak-Biran and Amiel [1].

----

*Fellow of the Alexander von Humboldt-Stiftung, Bonn

Table 1: Fractional cumulative yields (YFC) of several krypton and xenon isotopes in the fission of ^{232}Th by reactor neutrons ($T½$ = Half life)

Isotope	T½ (s)	YFC this work	YFC [1]
^{91}Kr	8.57	0.84±0.02	0.84±0.04
^{92}Kr	1.85	0.58±0.04	-
^{93}Kr	1.29	0.27±0.01	-
^{139}Xe	39.7	0.95±0.01	0.98±0.04
^{140}Xe	13.6	0.89±0.02	0.85±0.04
^{141}Xe	1.72	0.55±0.05	-
^{142}Xe	1.24	0.35±0.01	-
^{143}Xe	0.83/0.3	0.11±0.04*	-

*This value represents a lower limit as it can not be excluded that a non-negligible fraction of the ^{143}Xe decayed prior to emanation due to its short half life.

An analysis of all of the fission yields known for the reactor neutron induced fission of ^{232}Th using the systematics of Wahl [2] led to the following results concerning the model parameters:

$$\Delta Z(A'=140) = -\,0{,}45 \pm 0{,}01$$
$$\sigma_Z = 0{,}54 \pm 0{,}01$$
$$EOZ = 1{,}30 \pm 0{,}03$$
$$EON = 1{,}08 \pm 0{,}03$$
$$S = -\,0{,}004 \pm 0{,}004$$

The symbols used above represent the following parameters: $\Delta Z(A'=140)$ = Charge polarization at scission for the fragment mass A'=140; σ_Z = Width parameter of the Gauss'ian charge distribution curve; EOZ and EON = Even-odd pairing factors for protons and neutrons, respectively; and S parameter describing the mass dependence of ΔZ.

The analysis confirms in particular the high value of EOZ = 1.30 ± 0,12 of Izak-Biran and Amiel [1] on an extended data basis.

The present work is described in detail in a forthcoming paper [3].

References

[1] T. Izak-Biran and S. Amiel, Phys. Rev. C 16, 266 (1977)

[2] A.C. Wahl, Atomic Data and Nuclear Data Tables, in press.

[3] A. Srivastava and H. O. Denschlag, Radiochimica Acta, in press.

FRM-REAKTORSTATION GARCHING, FACHBEREICH PHYSIK
TECHNISCHE UNIVERSITÄT MÜNCHEN

1. Coherent Neutron Scattering Length and Total Cross Sections

1.1 Interactions of Slow Neutrons with Nuclides of Tungsten

K. Knopf and W. Waschkowski

The coherent neutron scattering lengths and total cross sections of elemental and oxide samples of natural and isotopically enriched W are determined. From these results the following coherent scattering length, b, and absorptions at 0.0253 eV, σ_γ, were deduced:

$b(^{nat}W) = 4.86 \pm 0.02$ fm, $\sigma_\gamma = 17.3 \pm 0.5$ b,
$b(^{182}W) = 7.04 \pm 0.04$ fm, $\sigma_\gamma = 19.6 \pm 0.3$ b,
$b(^{183}W) = 6.59 \pm 0.04$ fm, $\sigma_\gamma = 10.5 \pm 0.2$ b,
$b(^{184}W) = 7.55 \pm 0.06$ fm, $\sigma_\gamma = 1.7 \pm 0.1$ b,
$b(^{187}W) = -0.73 \pm 0.04$ fm, $\sigma_\gamma = 38.5 \pm 0.8$ b.

By comparison with the resonance parameters, the incoherence and the potential radii are derived and discussed. The bound level on W-182 must be fitted with a scattering width of $g\Gamma^o{}_n = 161$ meV at $E_o = -94$ eV.

Published in Z. Naturforschung 42a (1987) 909

1.2 Scattering of Slow Neutrons on Thorium

W. Waschkowski, K. Knopf, L. Koester

We determined with Christiansen filter technique and transmission measurements for thorium the following quantities:

- the coherent scattering length $b = 10.31 \pm 0.04$ fm,
- the absorption cross section at 0.0253 eV $\sigma_\gamma = 7.31 \pm 0.09$ b,
- the potential radius $R' = 9.6 \pm 0.2$ fm.

In combination with the same scattering cross sections in the eV-energy region we got information of bound levels at negative energy.

Submitted to Z. Naturforschung

2. Integral Values

2.1 Experimental Study on p-Wave Neutron Strength Functions for Light Nuclei

L. Koester, W. Waschkowski, J. Meier, G. Rau, M. Salehi

Broad energy distributions in fast neutron beams have been achieved by appropriate filtering of the ^{236}U fission radiation provided from the RENT converter facility at the FRM research reactor. Transmission measurements in such beams result in the average cross sections to which resonance reactions and shape elastic scattering contribute.
We used a silicon (124.5 cm) filtered beam with a medium energy of 143 keV (width 20 keV) and beams with 1.3 MeV (0.55 to 3 MeV) and 2.1 MeV (1 to 5.5 MeV) obtained through different filter combinations of lead and polyethelene. The relative high energies and the broad spectra made it possible to determine experimentally the contributions of s- and p-wave resonance reactions to the average cross section even for light nuclei.
Using the three different beams we determined the average cross sections for the elements in the mass region A=9 to 65. Analyzing the measured cross sections by means of the R matrix formalism provided a complete set of p-wave strength functions and distant level parameters. Moreover, single particle shell effects in the cross sections were observed. In conclusion we obtained informations on the 2P and the 3S size resonances and about the validity of the optical model for neutron reactions with light nuclei.

Submitted to Z. Phys.A

3. Fundamental Research

3.1 Experimental Study on the Electric Polarizability of the Neutron

L. Koester, W. Waschkowski, J. Meier

Neutron transmission cross sections of lead and bismuth were measured for 143 keV and with high precision for 1970 eV neutrons wich were selected from the reactor neutron spectrum by means of a novel dual combination of resonance scatterers. These data and highly accurate values of the coherent scattering lengths at zero energy and of transmission cross sections at 1.26, 5.19, 18.8 and 132 eV were the basis to determine the potential scattering radii, the neutron-electron and the electric polarization scattering lengths as well as to test the used resonance corrections by which the influence of nuclear reactions on the results is eliminated. We obtained for the electric polarizability of the neutron: $\alpha_n = (0.8 \pm 1.0)\ 10^{-3}\ fm^3$ and for the neutron electron scattering length: $b_{ne} = (-1.32 \pm 0.04)\ 10^{-3}$ fm. In conclusion we have shown that these results favour the cloudy bag model for the description of the neutron's charge structure.

Published in Z. Phys. A329 (1988) 229

INSTITUT FÜR KERNENERGETIK UND ENERGIESYSTEME
UNIVERSITÄT STUTTGART

1. Evaluation of Neutron Cross-Sections for Liquid Hydrogen and Deuterium[1]

D. Emendörfer, J. Keinert, M. Mattes

Cross sections for slow neutron scattering from H_2 and D_2 have been calculated taking into account the liquid state. The ability of the model [2] is demonstrated by comparison with experimental results for differential and total cross sections [1] [2]. Our static structure factor has been approximated for low κ-values by a solution of the Percus-Yevick equation for hard spheres and for higher κ-values by a Fourier-Transformation of the low density pair distribution function with the Lenard-Jones potential for the interaction of the molecules.

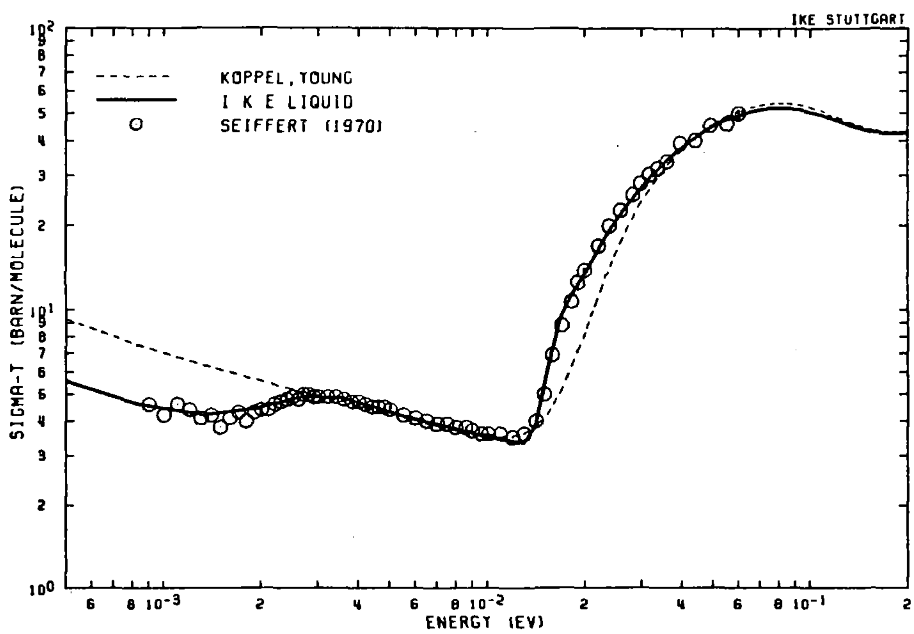

Total neutron cross sections for para-hydrogen at T = 14 K

References

[1] Keinert, J. and J. Sax: Investigation of Neutron Scattering Dynamics in Liquid Hydrogen and Deuterium for Cold Neutron Sources.
Kerntechnik 51 (1987), 19

[2] Bernnat, W., D. Emendörfer, J. Keinert, M. Mattes: Evaluation of Neutron Cross-Sections for Liquid Hydrogen and Deuterium for the Design of Cold Neutron Sources. Proc. Int. Conf. on Nuclear Data for Science and Technology, Mito/Japan, May 30 -June 3, 1988, in press

[1]funded by BMFT, Project 'Erforschung kondensierter Materie und Atomphysik'

2. Validation and Benchmark Testing of JEF-1

W. Bernnat, J. Keinert, D. Lutz, M. Mattes

For the validation and benchmark testing of JEF-1 group constants were produced with a modified and extended version of NJOY for nearly all JEF materials including minor actinides, fission products and thermal scattering matrices.
The group cross-section library comprises three partly overlapping ranges:

151 thermal groups from 0.00001 to 3.059 eV,
8500 resonance region groups from 0.876 eV to 4.3 keV (lethargy width 0.001),
100 groups between 0.414 eV and 14.98 MeV (GAM-II structure).

Calculations have been completed for a wide range of systems. The aims were
(a) to give an overall indication of the performance of JEF-1 to users of the library,
(b) to give guidance to the evaluators on data which should be reviewed for JEF-2,
(c) to intercompare different processing and calculational methods.
Overall the performance of the JEF-1 neutron interaction cross-section library is broadly satisfactory for the systems studied. Most of our JEF validation work has been reported [1] [2] [3].

The extensive series of calculations of thermal reactor benchmark experiments show the generally good performance of JEF-1. The only significant problem area is the overestimation of k_{eff} for the plutonium nitrate aqueous solutions. This is in contrast to the satisfactory agreement found for mixed UO_2 - PuO_2 lattices.

References:

[1] Bernnat, W., Mattes, M., Arshad M., Pohl B.: Analysis of Critical Experiments for the Validation of JEF-1 Data in Thermal Reactor Applications, Proc. Int. Topical Meeting on Advances in Reactor Physics, Mathematics and Computation, Paris, April 27-30, 1987

[2] Bernnat, W. et al.: Nuclear Criticality Safety Analysis based on the Joint Evaluated File JEF-1,
Proc. Int. Seminar on Nuclear Criticality Safety, Tokyo, Oct. 19-23, 1987

[3] Lutz, D.: Contributions to the HCLWR Cell Burn-up Benchmark, Specialists' Meeting on the NEACRP Burnup Benchmark Calculations for High Conversion Light Water Reactor Lattices, NEA Data Bank, Saclay, April 19-22, 1988

INSTITUT FÜR STRAHLENPHYSIK
UNIVERSITÄT STUTTGART

1. Coupled Channels and Microscopic Spherical Model Analysis of Polarized Neutron Scattering Data

W. Grum, J.W. Hammer, K.-W. Hoffmann, G. Schreder and G. Schleußner[1]

A coupled channels analysis has been performed for scattering of 7.75 MeV polarized neutrons on ^{nat}W, ^{nat}Pb, ^{209}Bi, ^{232}Th and ^{238}U. The detailed description of the SCORPION setup and the various methods of data evaluation can be found in reference [1]. The calculations carried out with the code ECIS79 revealed much better results when an imaginary spin-orbit term was included in the Woods-Saxon type model potentials. Illustrative results for thorium and uranium can be seen in figs. 1 and 2. The corresponding parameters are sampled in table 1.

Table 1: Neutron optical model parameters at $E_n = 7.75$ MeV. (MeV for depths, fm for geometry)

parameters	^{232}Th	^{232}Th	^{238}U	^{238}U
V_r	44.029	43.878	43.112	43.141
r_r	1.260	1.260	1.265	1.266
a_r	0.624	0.647	0.680	0.674
W_d	6.969	7.099	5.848	5.849
r_i	1.195	1.231	1.264	1.274
a_i	0.538	0.510	0.529	0.527
V_{so}	4.776	5.668	5.154	5.285
r_{so}	1.179	1.206	1.230	1.227
a_{so}	0.234	0.439	0.303	0.438
W_{so}	—	0.993	—	1.258
r_{wso}	—	1.206	—	1.227
a_{wso}	—	0.439	—	0.438
β_2	0.190	0.190	0.198	0.198
β_4	0.071	0.071	0.057	0.057
χ^2_{dwq}	76.1	74.8	31.6	29.2
χ^2_{ay}	102.6	36.6	58.3	20.0
χ^2/N	3.0	1.9	1.7	0.9
volume integrals				
J_v/A	392.6	393.0	392.7	393.4
$\langle r_v \rangle$	6.43	6.46	6.58	6.57
J_d/A	44.6	45.6	40.7	41.2
$\langle r_i \rangle$	7.66	7.84	8.12	8.18
$J_{so}/A^{1/3}$	141.5	171.8	159.3	163.0
$\langle r_{so} \rangle$	7.28	7.54	7.68	7.73
$J_{wso}/A^{1/3}$	—	30.1	—	38.8
$\langle r_{wso} \rangle$	—	7.54	—	7.73

[1] *deceased*

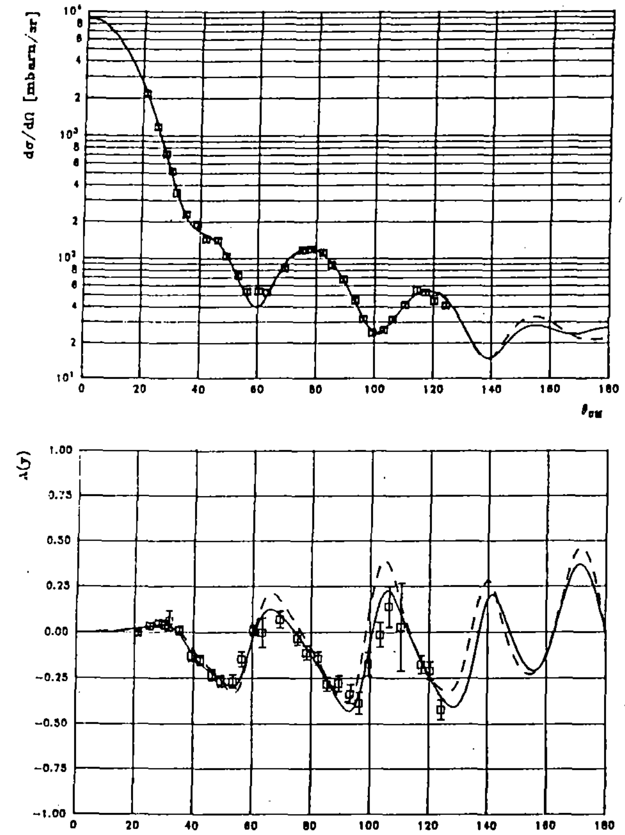

Figure 1: Differential cross section and analysing power angular distributions for ^{232}Th. The data are given together with the coupled channels results with(——) and without(- - -) an imaginary spin-orbit potential.

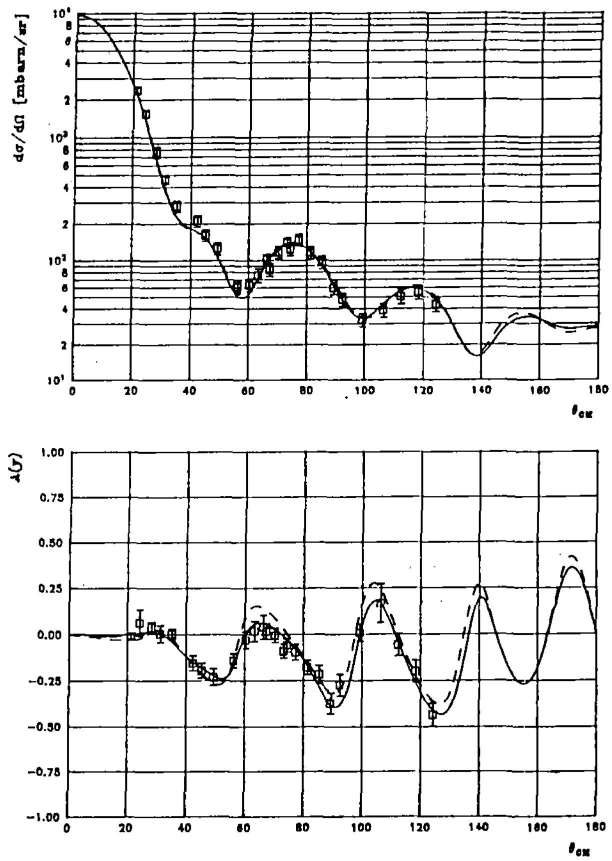

Figure 2: Differential cross section and analysing power angular distributions for ^{238}U. The data are given together with the coupled channels results with(——) and without(- - -) an imaginary spin-orbit potential.

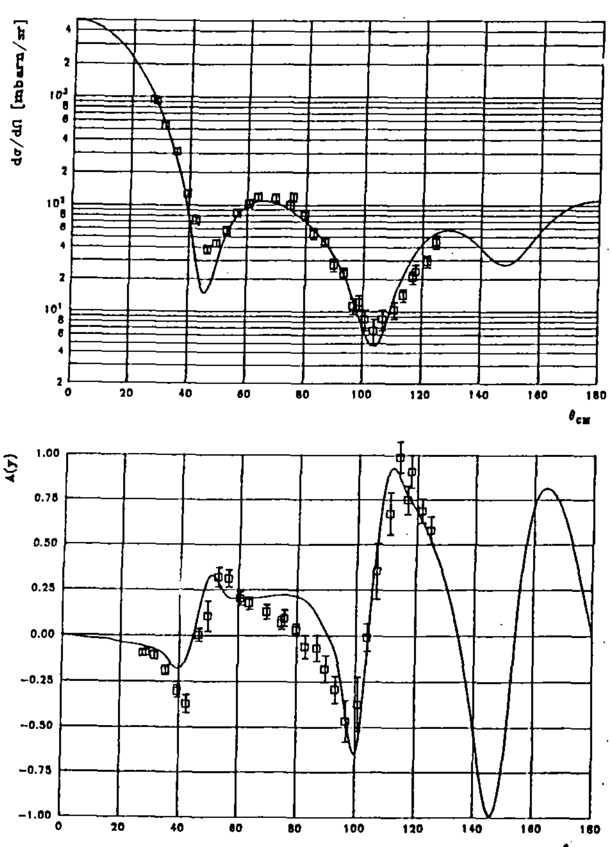

Figure 3: Differential cross section and analysing power angular distributions for ^{89}Y. The data are given together with the microscopic model results.

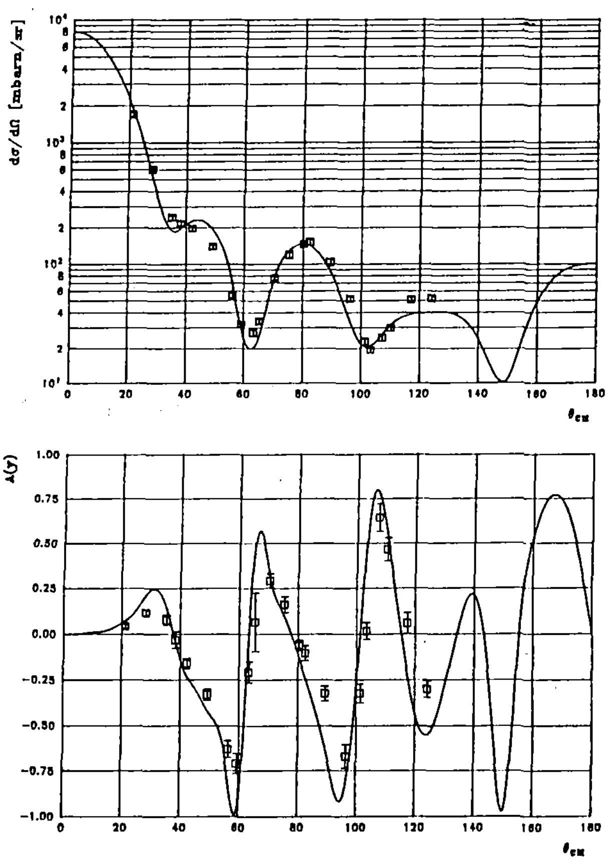

Figure 4: Differential cross section and analysing power angular distributions for ^{nat}Pb. The data are given together with the microscopic model results.

Differential cross section and analysing power data for ^{89}Y and ^{nat}Pb have been analysed with a microscopic potential of the Brieva-Rook-von Geramb type [2], which were provided in tabulated form [3]. Emphasizing the fact that the potentials were only renormalized without any change of geometry, they lead to quite promising model fits. See figs. 3 and 4 as well as table 2.

Table 2: Microscopic model parameters at $E_n = 7.75$ MeV.

nucleus	renormalization of potentials				data		χ^2_σ	$\chi^2_{A_y}$	χ^2/N
	λ_V	λ_W	$\lambda_{V_{so}}$	$\lambda_{W_{so}}$	$d\sigma/d\Omega$	A_y			
nat. Pb	1.17	0.504	2.58	-3.34	0.91	1.0	309	400	16.1
^{89}Y	1.15	0.510	1.81	-0.85	0.94	0.9	197	209	6.7

References

[1] J.W. Hammer, G. Bulski, W. Grum, W. Kratschmer, H. Postner, and G. Schleußner, NIM **244**, 455 (1986).

[2] H.V. von Geramb, F.A. Brieva, and J.R. Rook, in *Microscopic optical potentials*, Hamburg 1978, ed. H.V. von Geramb, Springer, Berlin, 1979.

[3] H.V. von Geramb, private communication, Mai 1985.

2. Coupled Channels Optical Model Analysis of Polarized Neutron Scattering Data for Al, Cu and Cr

G. Dagge, W. Grum, J.W. Hammer, K.-W. Hoffmann and G. Schreder

For the nuclei Al, Cu and Cr a polarized neutron scattering experiment has been performed using the Stuttgart SCORPION facility [1] to obtain the differential cross-section and the analyzing power at $E_n = 7.75$ MeV (Cu, Cr) and 7.62 MeV (Al) respectively. In all cases, the scattering samples contained the natural abundance ratios of the nuclei.

The data correction was done by applying the code XJANE [3] , which is a modification of the well known code JANE [2] . The modified code provides finite geometry- and multiple scattering corrections up to triple scattering sequences. For Cu and Cr, the multiple scattering effects are large, due to the large forward scattering and high nuclear density of these samples. In both cases a multiple- scattering correction which estimates the yields of higher scattering sequences was included [4] .

The subsequent coupled-channels analysis [5] showed that the nucleus aluminum could be explained excellently by the excited core model. (Fig. 1)
For scattering processes, Al can be treated as a silicon core and a weakly coupled $d_{5/2}$ proton hole, which has no influence on the elastic scattering but splits the excited states of silicon into a quintet without changing the shape of the inelastic cross-section. Since Si is known to be a rotator, a rotational $0^+/2^+$ coupling scheme with the deformation parameters of Si was used. This model, which was applicated by [6] to describe the differential cross-section at 11, 14 and 17 MeV, can now be confirmed down to 8 MeV and is also supported by the analysing power data of this work. The large compound cross-section at this energy was taken into account.
In the case of copper, the basic problem is to treat both isotopes ^{63}Cu and ^{65}Cu together. The geometric parameters of both nuclei are identical but the deformation parameters are not equal. Again, each isotope can be described in terms of the excited core model, in this case a $2p_{3/2}$-proton is coupled to a harmonic vibrational Ni-core [7] , [8] .
The quartets arising from this coupling of the proton to the first excited Ni-level could be observed, though unresolved. According to this model, it was possible to specify reduced nuclear matrix elements which allowed a simultaneous parameter-search for both isotopes. The best-fit (Fig. 2) indicates a successfull description of natural copper with this model.
The last nucleus under investigation is Cr. Compared to Cu, the situation here is less complicated since natural Cr contains 83 % of ^{52}Cr. Provided the excited core model holds also for ^{53}Cr , both isotopes should give similar scattering data.
^{52}Cr is conventionaly described as a vibrator. The parameter search is still in progress, although the model calculations agree already quite well with the measurements. Since the level scheme of Ni indicates an anharmonic vibrator, latest calculations are done with an anharmonic model, which provides a better representation of the data. (Fig. 3)

References

[1] J.W. Hammer, G. Bulski, W. Grum, W. Kratschmer, H. Postner, and G. Schleußner, NIM **244**, 455 (1986).

[2] E. Woye et al., Nucl.Phys. **A394**, 139 (1983).

[3] W. Grum, code XJANE, unpublished.

[4] R. C.Byrd, C. E. Floyd, R. L. Walter, Nuc. Phys. **A427** (1984) 36-60.

[5] J. Raynal, coupled-channel code ECIS79, 1979 (unpublished).

[6] C. S. Whisnant, J. H. Dave, C. R. Gould, Phys. Rev. **C30** (1984) 1435-1441.

[7] S. M. El-Kadi et al., Nuc. Phys. **A390** (1982) 509-540.

[8] J. P. Delaroche et al, Nuc. Phys. **A390** (1982) 541-560.

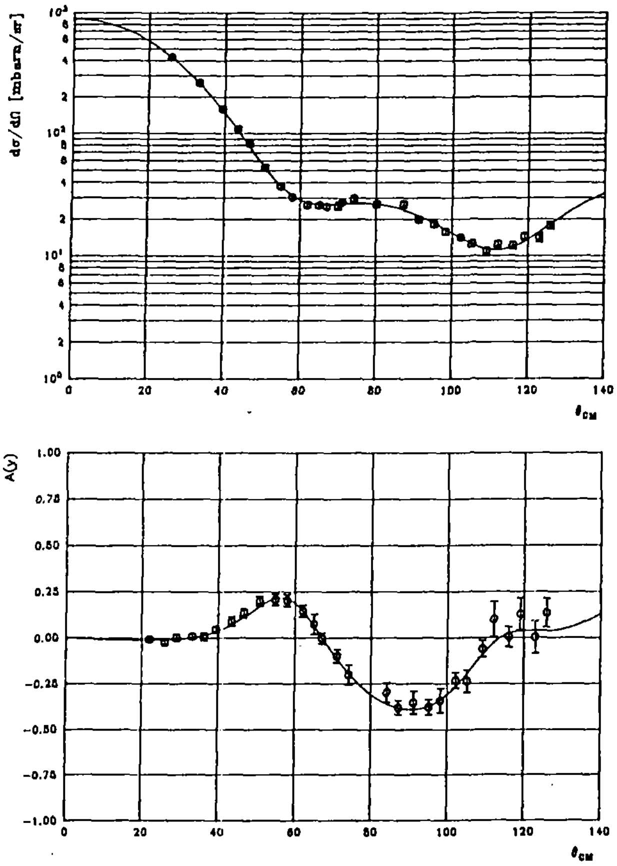

Fig. 1:
Experimental corrected data of elastic scattering on Al at 7.62 MeV compared with coupled channels analysis, differential cross-section and analysing power.

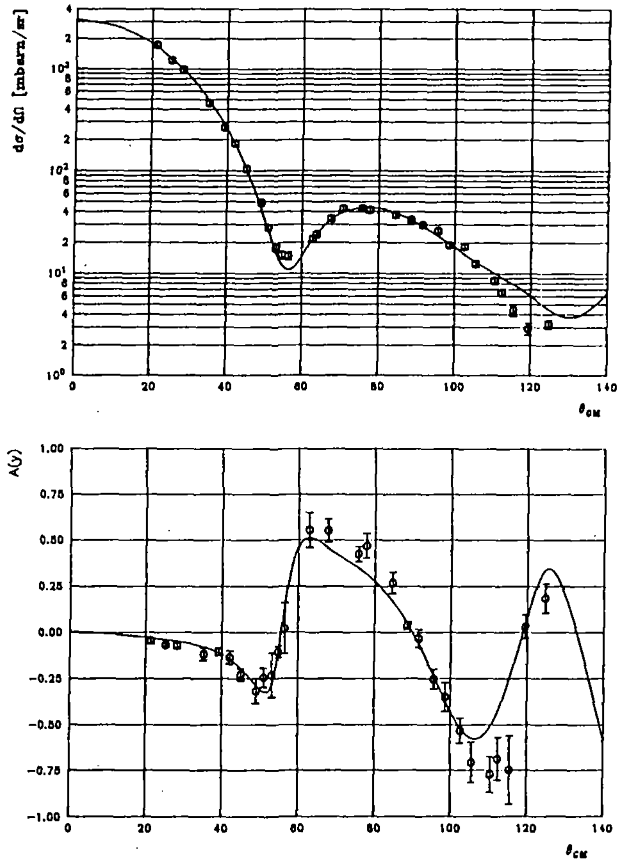

Fig. 2:
Experimental corrected data of elastic scattering on Cu at 7.75 MeV compared with coupled channels analysis, differential cross-section and analysing power.

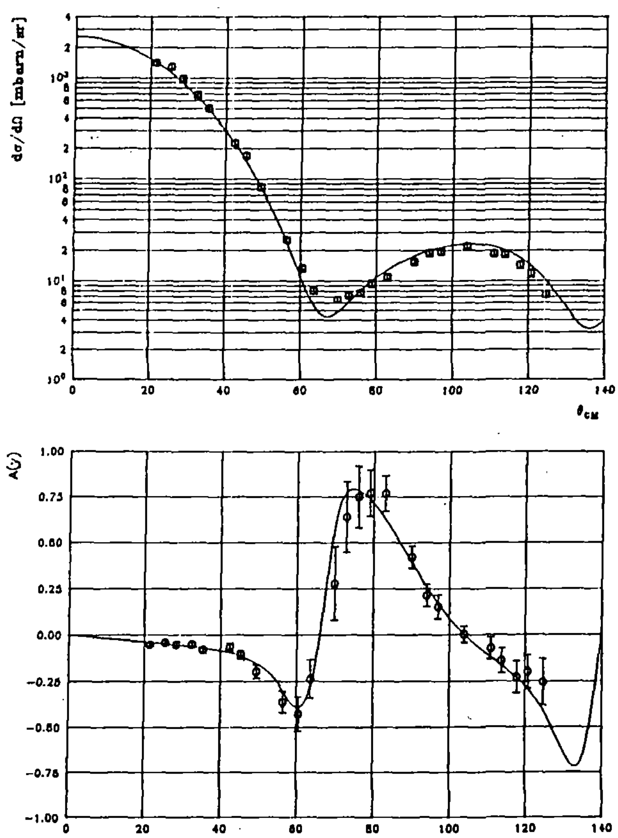

Fig. 3:
Experimental corrected data of elastic scattering on Cr at 7.75 MeV compared with coupled channels analysis, differential cross-section and analysing power.

3. Investigation of Neutron Producing Reactions in Stars: The $^{13}C(\alpha,n)^{16}O$ – Reaction

A. Köhler, G. Bulski and J.W. Hammer

In present models of stellar evolution some mixing of material of the hydrogen burning phase with material of the helium burning phase becomes possible due to instabilities, convection or rotation. In this way ^{12}C – produced in the triple $\cdot\alpha\cdot$ process – is converted via the chain $^{12}C(p,\gamma)^{13}N(e^+,\nu)^{13}C(\alpha,n)^{16}O$ (Q = 2.22 MeV) into ^{13}C, making its (α,n)-reaction a probable source of neutrons for the s-process. In the astrophysical s-process the elements with $A \geq 56$ are produced by neutron capture and successive β-decays in a "slow" time scale. Thus an improved knowledge of the behaviour of $^{13}C(\alpha,n)^{16}O$ at low α-energies is important for astrophysics. The reaction has been investigated with thick targets (about 200 keV) by Davids [1] in the range 475 - 700 keV and by Ramström and Wiedling [2] from 600 to 1150 keV. In the latter case neutron spectroscopy was not applied. The cross section is decreasing by nearly an order of magnitude every 100 keV, therefore a reinvestigation using improved methods is worthwile. In ^{17}O there are states at 6.972, 6.862 and 6.356 MeV, of which the two higher ones may lead to resonances in the neutron channel at about 660 and 800 keV. The state at 6.356 MeV is lying near the α-threshold and thus the high energy tail of a possible resonance may influence the cross section in the energy range of interest. According to a microscopic calculation of Descouvemont [3] for this reaction an increasing S-factor towards low energies will result from this behaviour.

The reaction $^{13}C(\alpha,n)^{16}O$ will be investigated using the high α-currents of the Stuttgart Dynamitron accelerator and enriched solid state targets - about 20 keV thick - on a thin watercooled backing, as it has been used for neutron polarization measurements [4], [5]. In a first experiment scintillation detectors with NE213 have been used for reasons of high efficiency and immediate availability. After unfolding of the proton recoil spectra an energy information with moderate resolution can be obtained. Detectors for higher resolution - using ^3He - are beeing developed. A preliminary result is shown in Fig. 1, assuming an isotropic angular distribution of the neutrons as a first approach. The cross section was measured between 450 and 2000 keV covering nearly 8 orders of magnitude. There was no indication for resonances at E_α = 660 and 800 keV. An increasing S-factor towards low energies ($E_\alpha \leq 500$ keV) cannot be excluded nor confirmed with the present data. The investigation will be continued.

References

[1] C.N. Davids, Nucl. Phys. **A110**, 619 (1968).

[2] E. Ramström, and T. Wiedling, Astroph. J. **211**, 223 (1977), Nucl. Phys. **A272**, 259 (1976).

[3] P. Descouvemont, Phys. Rev. **C36**, 2206 (1987).

[4] J.W. Hammer, G. Bulski, W. Grum, W. Kratschmer, H. Postner, and G. Schleußner, NIM **244**, 455 (1986).

[5] W. Weiß, W. Grum, M. Koch, G. Schreder, and J.W. Hammer, Progr. Rep. NEANDC(E)-282 U Vol. V, INDC(Ger)-30/LN + Special, pp. 46, ed. S. Cierjacks and H. Behrens, Karlsruhe, 1988.

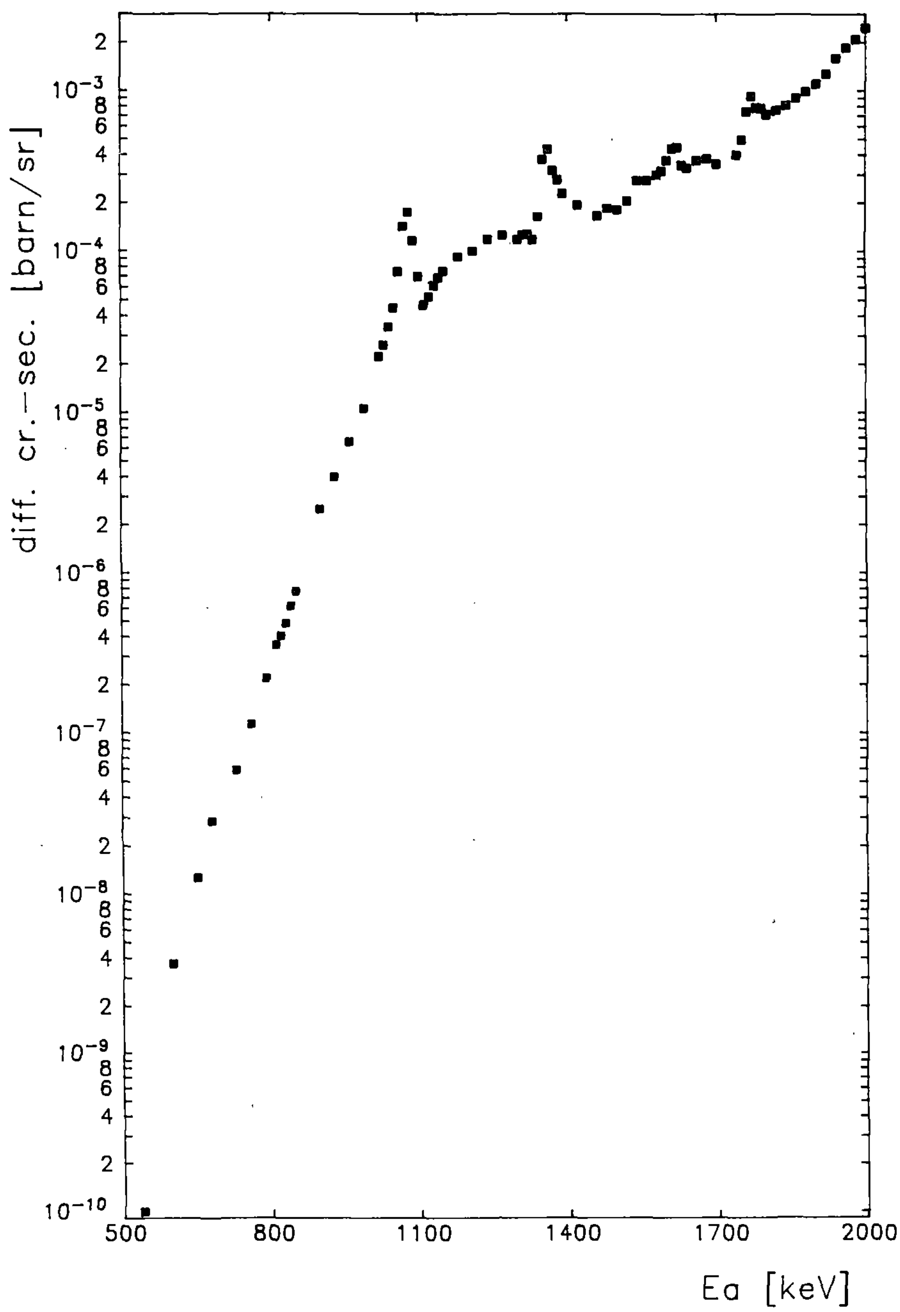

Figure 1: Differential cross section of $^{13}C(\alpha,n)^{16}O$ measured with a 4"Ø × 2" NE213–detector under 30° in close geometry. The target thickness was about 20 keV, the He^{+}–currents ranged from 50–120 μA. E_α is given in the laboratory system.

PHYSIKALISCH-TECHNISCHE BUNDESANSTALT
BRAUNSCHWEIG

1. Neutron Data

1.1 Measurement of the $^{27}Al(n,\alpha)$ and $^{24}Mg(n,p)$ Cross Sections Between 8 MeV and 15 MeV

G. Börker, H. Klein, W. Mannhart, M. Wagner*, G. Winkler*

By means of deuterons impinging on a deuterium gas cell, 'monoenergetic' neutrons between 8.3 MeV and 14.8 MeV were generated with the $D(d,n)^3He$ reaction. Samples of aluminum and magnesium were irradiated at a distance of 9 cm from the neutron target. The samples were placed back-to-back to a ^{238}U fission chamber acting as a neutron fluence monitor. Empty gas cell irradiations allowed the contribution of parasitic neutrons produced in the structural material of the gas cell to be subtracted. Simultaneously with the activation procedure, neutron time-of-flight spectra were recorded to determine the continuous neutron energy distribution of the D(d,np) break-up component and to correct its contribution to the activation process. The radioactivity of the samples was measured with a germanium detector calibrated against a large sodium iodide well-type detector.

Relative to $^{238}U(n,f)$, the excitation functions of $^{27}Al(n,\alpha)^{24}Na$ and $^{24}Mg(n,p)^{24}Na$ were determined in steps of 0.25 MeV. The analysis has not yet been completed.

1.2 Cf-252 Spectrum-Averaged Cross-Sections

W. Mannhart

Based on the recently evaluated shape of the Cf-252 neutron spectrum [1], average cross sections of neutron activation reactions, important in reactor metrology, were calculated. The results are listed in Table I. The energy-dependent cross section data used in this calculation were mainly taken from ENDF/B-V. Data from other sources are indicated in Table I with an additional reference. The calculated data are compared with data obtained from an extensive evaluation of the experimental data

---
*Institut für Radiumforschung und Kernphysik, Wien

Table I: Cf-252 spectrum-averaged neutron cross sections (in millibarn)

REACTION	CALCULATION		EXPERIMENT	RSD	C/E
F-19(N,2N)	1.714E-2*	[3]	1.613E-2	3.40	1.063
MG-24(N,P)	2.101E+0	[4]	1.998E+0	2.42	1.052
AL-27(N,P)	5.027E+0		4.885E+0	2.14	1.029
AL-27(N,A)	1.034E+0		1.017E+0	1.47	1.017
	9.886E-1	[5]			0.972
S-32(N,P)	7.591E+1		7.262E+1	3.50	1.045
TI-46(N,P)	1.317E+1		1.409E+1	1.76	0.935
TI-47(N,P)	1.933E+1	[6]	1.929E+1	1.66	1.002
	2.406E+1				1.247
TI-48(N,P)	4.002E-1		4.251E-1	1.89	0.941
V-51(N,P)	6.638E-1	[7]	6.493E-1	1.95	1.022
V-51(N,A)	3.878E-2	[8]	3.904E-2	2.22	0.993
MN-55(N,2N)	4.623E-1		4.079E-1	2.34	1.133
FE-54(N,P)	8.790E+1		8.692E+1	1.34	1.011
FE-56(N,P)	1.374E+0		1.466E+0	1.77	0.937
NI-58(N,P)	1.134E+2		1.176E+2	1.30	0.964
NI-58(N,2N)	9.048E-3	[9]	8.961E-3	3.59	1.010
	8.103E-3				0.904
CO-59(N,P)	1.699E+0	[10]	1.692E+0	2.49	1.004
CO-59(N,A)	2.110E-1		2.220E-1	1.86	0.950
CO-59(N,2N)	4.266E-1		4.055E-1	2.52	1.052
CU-63(N,G)	9.673E+0		1.045E+1	3.24	0.926
CU-63(N,A)	6.581E-1	[11]	6.893E-1	1.98	0.955
	7.383E-1				1.071
CU-63(N,2N)	2.082E-1	[4]	1.845E-1	3.98	1.128
CU-65(N,2N)	6.766E-1		6.587E-1	2.24	1.027
ZN-64(N,P)	3.913E+1	[4]	4.063E+1	1.64	0.963
ZR-90(N,2N)	2.196E-1	[4]	2.212E-1	2.90	0.993
IN-115(N,G)	1.217E+2		1.257E+2	2.23	0.968
IN-115(N,N')	1.834E+2		1.976E+2	1.37	0.928
I-127(N,2N)	2.349E+0		2.071E+0	2.75	1.134
AU-197(N,G)	7.619E+1		7.686E+1	1.59	0.991
AU-197(N,2N)	5.648E+0		5.511E+0	1.83	1.025
U-235(N,F)	1.237E+3		1.210E+3	1.20	1.022
NP-237(N,F)	1.360E+3		1.361E+3	1.58	0.999
U-238(N,F)	3.158E+2		3.257E+2	1.63	0.970
PU-239(N,F)	1.794E+3		1.812E+3	1.37	0.990

RSD : RELATIVE STANDARD DEVIATION IN %

*Read as 1.714×10^{-2}

base available [2]. The relative standard deviations of these experimental data are given. The comparison of the calculated data with the experimental data, shown in the last column of Table I, indicates that for most reactions an agreement between experiment and calculation is given within 5 % and confirms the suitability of these reactions for neutron spectrum unfolding purposes.

The quotation of uncertainties corresponding to the calculated data has been postponed due to the fact that some of the existing covariance files of $\sigma(E)$ data seem to be rather unrealistic.

1.3 Characteristics of the p + Be Neutron Producing Reaction

H.J. Brede, G. Dietze, U.J. Schrewe, F. Tancu*, C. Wen+

Neutron yields of a thick Be target were investigated for proton energies between 17 and 22 MeV. The spectral neutron yield per unit beam charge on the Be target was determined with time-of-flight techniques by using the pulsed beam of a cyclotron, a flight path of 20 m and the (n,γ) discrimination properties of an NE213 scintillation detector. In addition, the angular dependence of the spectral yield was measured between 0 and 135 degrees neutron emission angle for a proton energy of 19.1 MeV.

The actual neutron spectra differ in the low-energy region from those published by Lone et al. [12] and deviations of up to 20 % (see Fig. 1) in the total neutron yield per unit beam charge at 0 degrees as a function of the incident proton energy were found [13].

1.4 Q Values for (p,n) Reactions on ^{65}Cu and ^{51}V

H. Schölermann, R. Böttger

Combining a time-of-flight method for the determination of neutron energy with a precise measurement of the energy of the incident protons results in a high accuracy of the Q values.

---

* Institute of Nuclear Physics and Engineering, Bucharest, Rumania

+ Beijing Normal University, Beijing, People's Republic of China

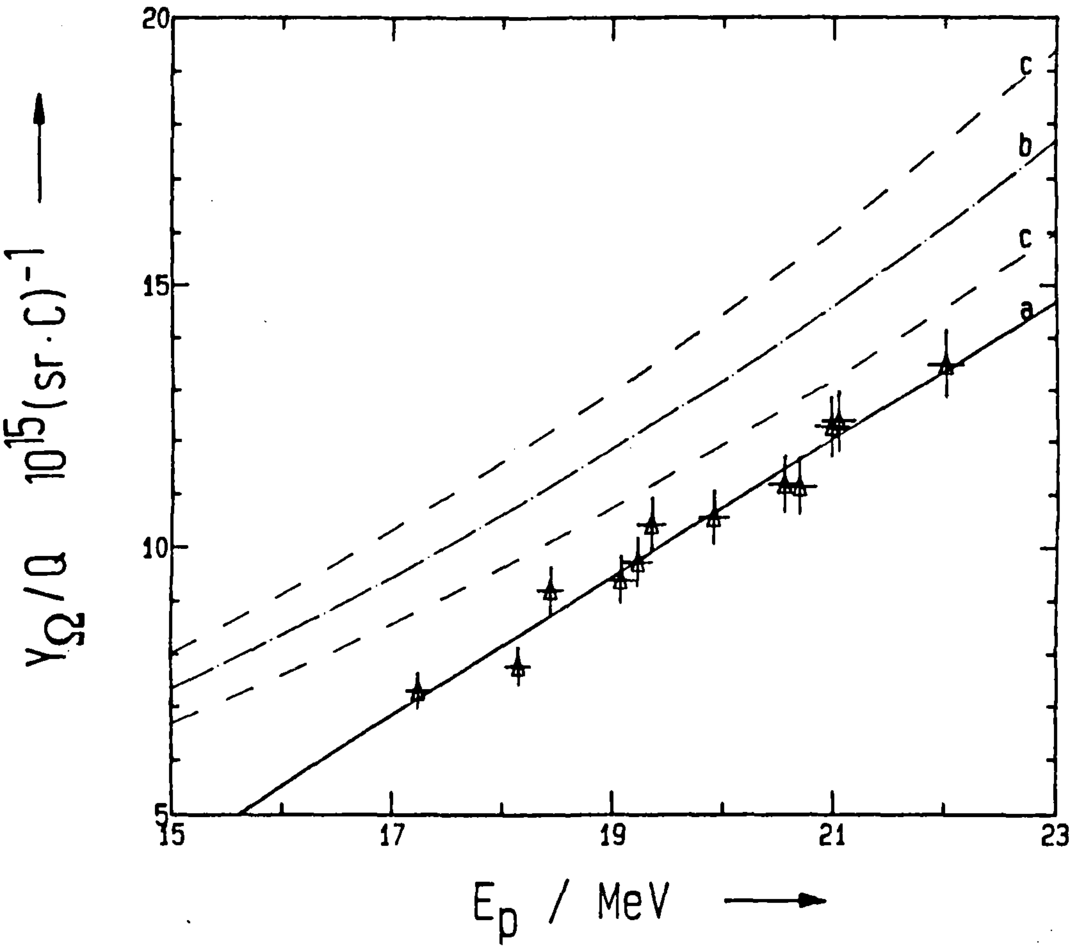

Fig. 1 Neutron yield per unit beam charge, Y_Ω/Q, of a thick Be target at zero degrees as a function of proton energy, E_p, with a neutron energy threshold of 2 MeV. The data points (Δ) represent the actual measurements. Curve (a) corresponds to a least-squares fit. Curve (b) represents Lone's function [12] and curve (c) its 1σ confidence limit.

In the first experiment a thin layer of the target material evaporated on a tantalum backing is bombarded with a pulsed proton beam of the PTB's 3.8 MeV Van de Graaff accelerator. As the proton energy is chosen about 50 keV above the threshold energy, every resonance between the energy of the incident protons and the threshold is excited due to the energy loss in the material.

The emitted neutrons were detected by a 25.4 Ø x 6.4 mm Li glass scintillator 200 mm behind the target. To define the effective centre of the detector, the measured peak forms were compared with computer calculations which included the time

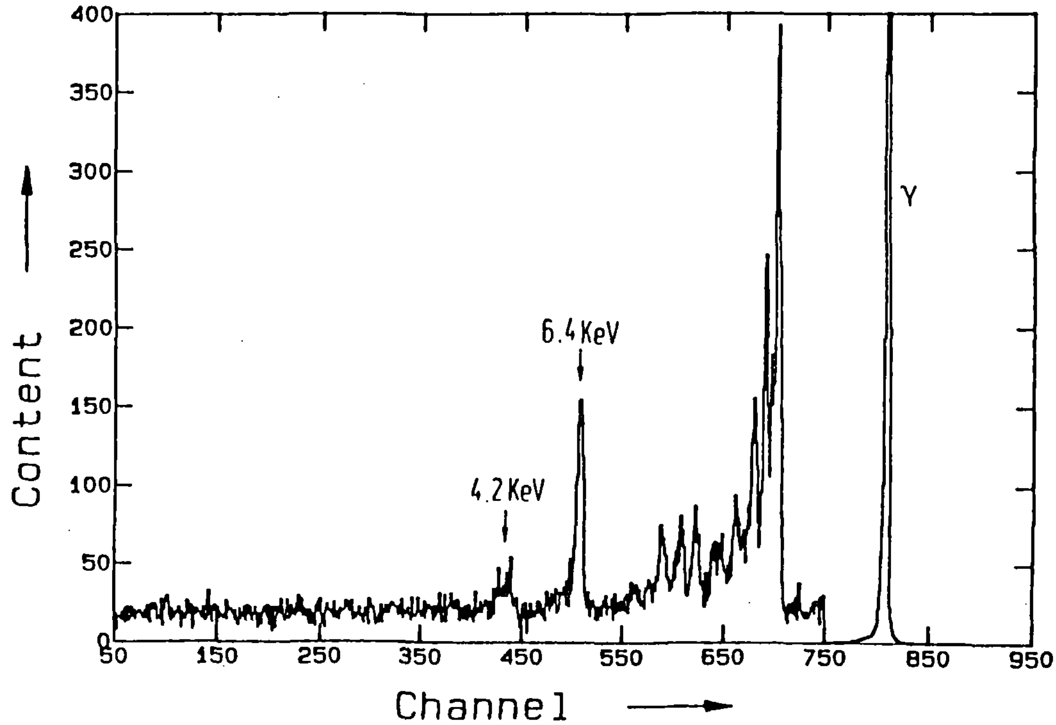

Fig. 2 Time-of-flight spectrum of the neutron yield per incident beam charge from $^{51}V(p,n)^{51}Cr$ for proton energy near the threshold.

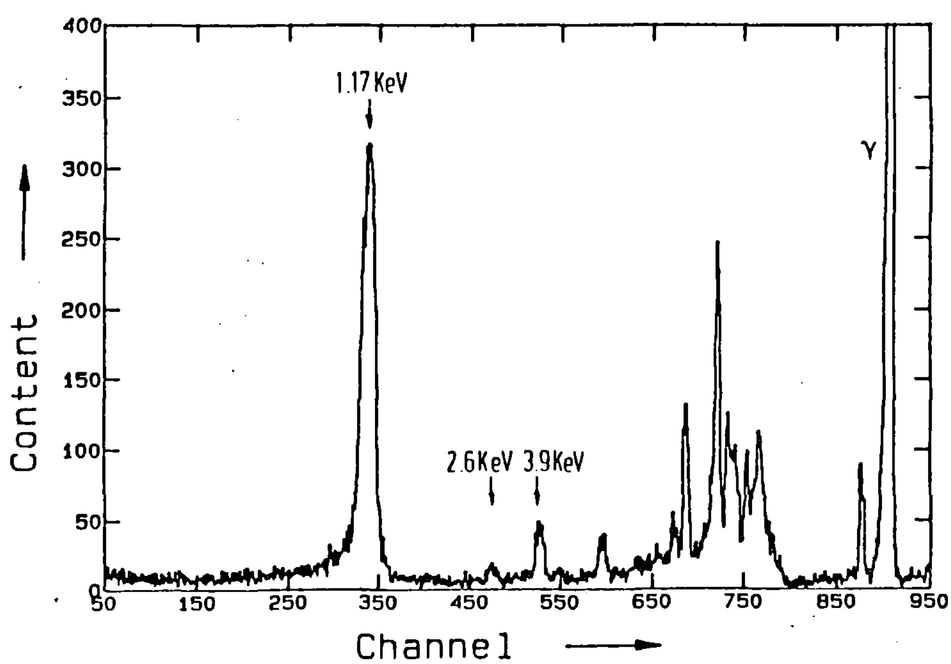

Fig. 3 Time-of-flight spectrum of the neutron yield per incident beam charge from $^{65}Cu(p,n)^{65}Zn$ for proton energy near the threshold.

structure of the proton beam, the size of the detector, neutron absorption and first-order scattering in the detector. Figs. 2 and 3 show the time-of-flight spectra for $^{51}V(p,n)$ and $^{65}Cu(p,n)$ near the threshold.

In the second experiment the targets were bombarded with an unpulsed proton beam of high-energy resolution several keV above a pronounced (p,n) resonance. A positive high voltage of 0 - 20 kV controlled by a ramp generator with a linearly increasing slope and a period of 50 s was applied to the target.

Increasing the voltage at the target decreases the energy of the protons. As long as the proton energy is above the threshold, the neutron yield is high. The decrease in the neutron count rate indicates the position of the resonance. The advantage of this procedure is that the calibrated Van de Graaff - the calibration is performed using the well known $Al(p,\gamma)$ resonances and the threshold of $^{7}Li(p,n)$ and $^{13}C(p,n)$ - is left untouched, together with all the elements of the beam line system, and small energy changes are performed only by wobbling the target voltage.

An extensive covariance analysis was carefully carried out. A data field of more than 100 parameters with their uncertainties and correlations was taken into account. The results obtained from these investigations are:

$$Q_{Cu} = -2.13355 \pm 0.00043 \text{ MeV}$$
$$Q_{V} = -1.53511 \pm 0.00024 \text{ MeV}$$

The pronounced resonance in the time-of-flight spectrum of the $^{65}Cu(p,n)$ reaction (Fig. 3) has recently been used as an appropriate source of 1.17 keV neutrons in our laboratory.

2. Radionuclide Data

2.1 Half-Lives

H. Schrader, K.F. Walz

The half-lives of the radionuclides ^{18}F and ^{201}Tl were determined by following the decay of the radioactive substance with a pressurized 4π ionization chamber. A source consisted of a 2 ml radioactive solution in a sealed glass ampoule. The sources were examined for impurities by germanium detector measurements. The stability of the chamber was checked by measurements of a radium reference source at the beginning and at the end of each measuring cycle. The data have been evaluated by least-squares fits and details of the data evaluation and results have been published [14]. The results for the radionuclides are summarized in Table II. The given uncertainties (in parentheses) correspond to one standard deviation and include systematic uncertainties. The half-life of ^{201}Tl has been remeasured since 1979 [15] and a revised value is given. The half-lives of ^{56}Co, ^{125}I [16] and ^{195}Au [17] have been published in previous reports. A publication dealing with these five radionuclides is in preparation. Measurements with sources of the radionuclides ^{85}Kr, ^{90}Sr, ^{108}Am^{m}, ^{133}Ba, ^{152}Eu and ^{154}Eu are being continued. It is hoped to achieve a total uncertainty of better than 0.1 %.

Table II: Half-lives

Nuclide	Duration of measurements in multiples of $T_{1/2}$	$T_{1/2}$
^{18}F	8.7	109.70 (11) min
^{201}Tl	8.1	3.043 (3) d

References

[1] Mannhart, W., "Evaluation of the Cf-252 fission neutron spectrum between 0 MeV and 20 MeV", in Properties of Neutron Sources (Proc. Advisory Group Meeting, Leningrad, USSR, 1986), IAEA-TECDOC-410, IAEA, Vienna (1987) 158

[2] Mannhart, W., in Reactor Dosimetry (Proc. 5th ASTM-Euratom Symp., Geesthacht, F.R.G., 1984) (Genthon, J.P. and Röttger, H., Eds.) Reidel, Dordrecht (1985) 801

[3] Strohmaier, B., Tagesen, S., Vonach, H., Phys. Data 13-2 (1980)

[4] Tagesen, S., Vonach, H., Strohmaier, B., Phys. Data 13-1 (1979)

[5] Tagesen, S., Vonach, H., Phys. Data 13-3 (1981)

[6] Mannhart, W., Smith, D.L., Meadows, J.W. in Nuclear Data for Basic and Applied Science (Proc. Int. Conf., Santa Fe, N. Mex., 1985) (Young, P.G. ed.) Gordon and Breach, New York (1986) 577

[7] Smith, D.L., Meadows, J.W., Kanno, I., "Measurement of the V-51(n,p) reaction cross section from threshold to 9.3 MeV by the activation method", Argonne National Laboratory, Ill,, Rep. ANL/NDM-85 (June 1984)

[8] Kanno, I., Meadows, J.W., Smith, D.L., "Energy-differential cross section measurement for the V-51(n,) reaction", Argonne National Laboratory, Ill., Rep. ANL/NDM-86 (July 1984)

[9] Pavlik, A., Winkler, G., "Evaluation of the Ni-58(n,2n) cross-section", IAEA, Vienna, Rep. INDC(AUS)-9/L (1983)

[10] Smith, D.L., Meadows, J.W., Nucl. Sci. Eng. 60 (1976) 187

[11] Winkler, G., Smith, D.L., Meadows, J.W., Nucl. Sci. Eng. 76 (1980) 30

[12] Lone, M.A., Ferguson, A.J., Robertson, B.D., Nucl. Instrum. Meth. 189 (1981) 515

[13] Brede, H.J., Dietze, G., Kudo, K., Schrewe, U.J., Tancu, F., Wen, C. (to be published in Nucl. Instrum. Meth.)

[14] Walz, K.F., Debertin, K., Schrader, H, Int. J. Appl. Radiat. Isot. 34 (1983) 1191

[15] Walz, K.F., Debertin, K., Schötzig, U., NEANDC (E)-202 U, Vol. V (1979) 84

[16] Schrader, H., Walz, K.F., NEANDC (E)-282 U, Vol. V (1987) 56

[17] Schrader, H., Walz, K.F., NEANDC (E)-272 U, Vol. V (1986) 49

FACHINFORMATIONSZENTRUM
ENERGIE PHYSIK MATHEMATIK GMBH

Status Report

H. Behrens, H.-W. Müller

1. Data Compilations

The following new issue has been published in our series PHYSICS DATA:

A. Pavlik and H. Vonach
Evaluation of the angle integrated neutron emission cross sections from the interaction of 14 MeV neutrons with medium and heavy nuclei
PHYSICS DATA 13-4 (1988)

2. Evaluated Nuclear Structure and Decay Data

Nuclear structure and decay data are evaluated by an international network of evaluation centers under the auspices of the International Atomic Energy Agency (IAEA).
The Fachinformationszentrum Karlsruhe (FIZ) has the responsibility for the evaluation of the mass range A = 81 - 100. The evaluations are published as "Nuclear Data Sheets". The computerized version is the Evaluated Nuclear Structure Data File (ENSDF) which covers the mass range A = 1 - 263. A special representation of radioactivity data for application purposes is the file MEDLIST. Data from both files can be retrieved either online or on request from the Fachinformationszentrum (FIZ).

Updates of ENSDF:

ENSDF and MEDLIST were updated in May and October. 31 mass chains have been re-evaluated in 1987.

Current contents:

ENSDF: 2,363 nuclides

10,077 data sets (each representing a special type of experiment, or ADOPTED LEVELS, GAMMAS properties)

749,825 records (of 80 byte)

MEDLIST: 2,262 data sets (each representing one decay mode of a radionucleus)

92,784 records

Status of mass chain evaluations of FIZ (A = 81 -100) from 1.4.87 to 31.3.88:

A = 88, 93	finished, in print
A = 86, 89	finished, in review
A = 84, 85, 87	in progress

References

Nuclear Data Sheets for A=88
H.W. Müller
Nuclear Data Sheets 54 (1988)

Nuclear Data Sheets for A=93
H. Sievers
Nuclear Data Sheets 54 (1988)

3. Database GAMCAT

A new database GAMCAT has been created comprising the computerized versions of the "Catalog of Gamma Rays from Radioactive Decay" by U. Reus and W. Westmeier (At. Data Nucl. Data Tables 29, 1 and 29, 193 (1983)) and the "Catalog of Alpha Particles from Radioactive Decay" by W. Westmeier and A. Merklin (Physics Data 29-1 (1985)).
A convenient retrieval system allwoys the retrieval of gammas or alpha particles by several quantities, e.g. energy, half-life, intensity. Online access is possible at the Fachinformationszentrum Karlsruhe (FIZ).

Contents:

2,326 radionuclei
47,000 gamma rays
1,900 alpha particle branches

A P P E N D I X

Addresses of Contributing Laboratories

Institut für Kernphysik II
Director: Prof. Dr. A. Citron
Senior reporter: Dr. S. Cierjacks
Kernforschungszentrum Karlsruhe
Postfach 3640
7500 Karlsruhe

Institut für Kernphysik III
Director: Prof. Dr. G. Schatz
Senior reporter: Dr. F. Käppeler
Kernforschungszentrum Karlsruhe
Postfach 3640
7500 Karlsruhe

Institut für Neutronenphysik und Reaktortechnik
Director: Prof. Dr. G. Kessler
Senior reporter: Dr. F. Fröhner
Kernforschungszentrum Karlsruhe
Postfach 3640
7500 Karlsruhe

Institut für Chemie (1): Nuklearchemie
Director: Prof. Dr. G. Stöcklin
Senior reporter: Dr. S.M. Qaim
Kernforschungsanlage Jülich
Postfach 1913
5170 Jülich

Institut für Reaktorentwicklung
Director: Prof. Dr. R. Hecker
Senior reporter: Dr. D. Filges
Kernforschungsanlage Jülich
Postfach 1913
5170 Jülich

Zentraleinrichtung für Strahlenschutz
Head and senior reporter: Prof. Dr. H. Michel
Universität Hannover
Am Kleinen Felde 30
3000 Hannover 1

Abteilung Nuklearchemie
Director: Prof. Dr. G. Stöcklin
Senior reporter: Dr. U. Herpers
Universität zu Köln
Zülpicher Str. 47
5000 Köln 1

Institut für Kernchemie
Director: Prof. Dr. G. Herrmann
Senior reporter: Prof. Dr. H.O. Denschlag
Universität Mainz
Fritz -Strassmann-Weg 2
6500 Mainz

Fachbereich Physik der
Technischen Universität München
Abteilung E14, Forschungsreaktor
Director: Prof. Dr. L. Köster
Senior Reporter: Dr. W. Waschkowski
8046 Garching/München

Institut für Kernenergetik und Energiesysteme
Director: Prof. Dr. A. Schatz
Senior reporter: DP M. Mattes
Universität Stuttgart
Almandring 3
7000 Stuttgart 80

Institut für Strahlenphysik
Director: Prof. Dr. K.W. Hoffmann
Senior reporter: Dr. J.W. Hammer
Universität Stuttgart
Almandring 3
7000 Stuttgart 80

Physikalisch-Technische Bundesanstalt
Abteilung 6, Atomphysik
Director: Prof. Dr. S. Wagner
Bundesallee 100
3300 Braunschweig

Fachinformationszentrum Energie, Physik, Mathematik
Directors: Dr. W. Rittberger, E.-O. Schulze
Senior reporter: Dr. H. Behrens
Kernforschungszentrum
7514 Eggenstein-Leopoldshafen